Energy Reports 8 (2022) 7154–7175

Contents lists available at ScienceDirect

Energy Reports

journal homepage: www.elsevier.com/locate/egyr

Research paper

An optimal sizing framework for autonomous photovoltaic/hydrokinetic/hydrogen energy system considering cost, reliability and forced outage rate using horse herd optimization

Abdulaziz Alanazi [a], Mohana Alanazi [b], Saber Arabi Nowdeh [c], Almoataz Y. Abdelaziz [d], Adel El-Shahat [e,*]

[a] Department of Electrical Engineering, College of Engineering, Northern Border University, Ar'Ar 73222, Saudi Arabia
[b] Department of Electrical Engineering, College of Engineering, Jouf University, Sakaka 72388, Saudi Arabia
[c] Institute of Research Sciences, Power and Energy Group, Johor Bahru, Malaysia
[d] Faculty of Engineering and Technology, Future University in Egypt, Cairo 11835, Egypt
[e] Energy Program, School of Engineering Technology, Purdue University, West Lafayette, IN 47907, USA

ARTICLE INFO

Article history:
Received 26 February 2022
Received in revised form 23 April 2022
Accepted 18 May 2022
Available online 2 June 2022

Keywords:
Hybrid PV/HKT/FC system
Sizing framework
Cos of energy
Probability of load supply
Forced outage concept
Horse herd optimization

ABSTRACT

The components outage of an energy system weakens its operation probability, which can affect the sizing of that system. An optimal sizing framework is presented for an autonomous hybrid photovoltaic/hydrokinetic/fuel cell (PV/HKT/FC) system with hydrogen storage to supply an annual load demand with forced outage rate (FOR) of the clean production resources based on real environmental information such as irradiance, temperature, and water flow. The sizing problem is implemented with the objective of cost of energy (COE) minimization and also satisfying probability of load supply (PLS) as a reliability constraint. The FOR effect of the photovoltaic and hydrokinetic resources is evaluated on the hybrid system sizing, energy cost, reliability, and also storage contribution of the system. Meta-heuristic horse herd optimization (HHO) algorithm with perfect capability on exploration and exploitation phases is used to solve the sizing problem. The results proved that the PV/HKT/FC configuration is the optimal option to supply the demand of an autonomous residential complex with the minimum COE and maximum PLS compared with the other system configurations. The results demonstrated the overlap of hydrogen storage with clean production resources to achieve an economic-reliable power generation system. The findings indicated that the COE is increased and the PLS is decreased due to the FOR increasing because of reducing the generation resources operational probability. The results demonstrated that the hydrogen storage level is increased with FOR increasing to maintain the system reliability level. Also, the sizing results indicated that the FOR of the hydrokinetic is more effective than the photovoltaic resources in increasing the system cost and undermining the load reliability. In sizing of the hybrid PV/HKT/FC system, the COE is obtained 1.57 $/kWh without considering the FOR and is achieved 1.66 and 1.63 $/kWh considering the FOR (8%) for the hydrokinetic and photovoltaic resources, respectively. Moreover, the results cleared that the HHO is superior in comparison with particle swarm optimization (PSO), genetic algorithm (GA), and grey wolf optimizer (GWO) in the PV/HKT/FC system sizing with the lowest COE and higher reliability.

1. Introduction

The increasing need for electrical energy and environmental pollution have faced the energy industry with the challenge of meeting energy needs as well as maintaining the level of reliability at the desired level (Adefarati and Bansal, 2017; Pepermans et al., 2005). One of the most important solutions to overcome these challenges, which has received much attention in recent years, is the application of distributed generation (DG) resources in power systems (Adefarati and Bansal, 2017; Pepermans et al., 2005; García et al., 2021). In a hybrid energy system consisting of different generation sources to supply the energy required by consumers, it is necessary to determine the optimal sizing of each of the different sources considering economic (cost) and technical (reliability) indices (Anoune et al., 2018; Lian et al.,

* Corresponding author.
E-mail addresses: af.alanazi@nbu.edu.sa (A. Alanazi), msanazi@ju.edu.sa (M. Alanazi), arabi.energy18@gmail.com (S. Arabi Nowdeh), almoatazabdelaziz@hotmail.com (A.Y. Abdelaziz), asayedah@purdue.edu (A. El-Shahat).

https://doi.org/10.1016/j.egyr.2022.05.161

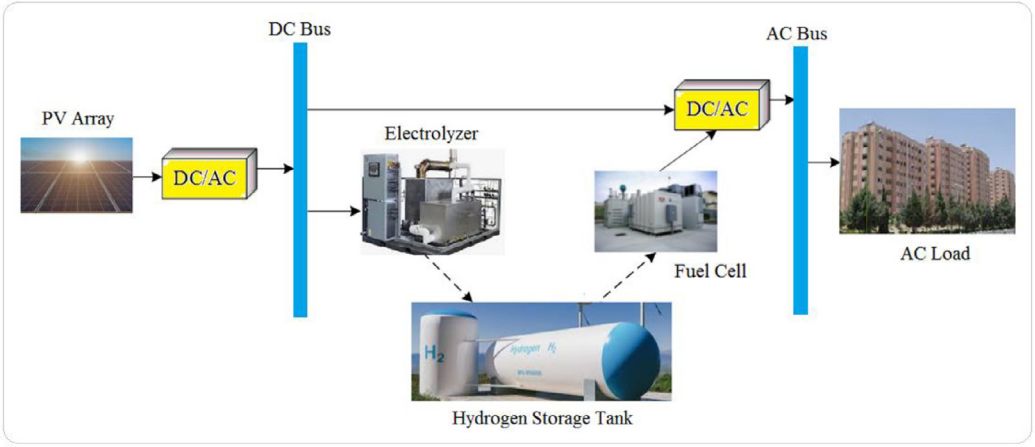

(a)

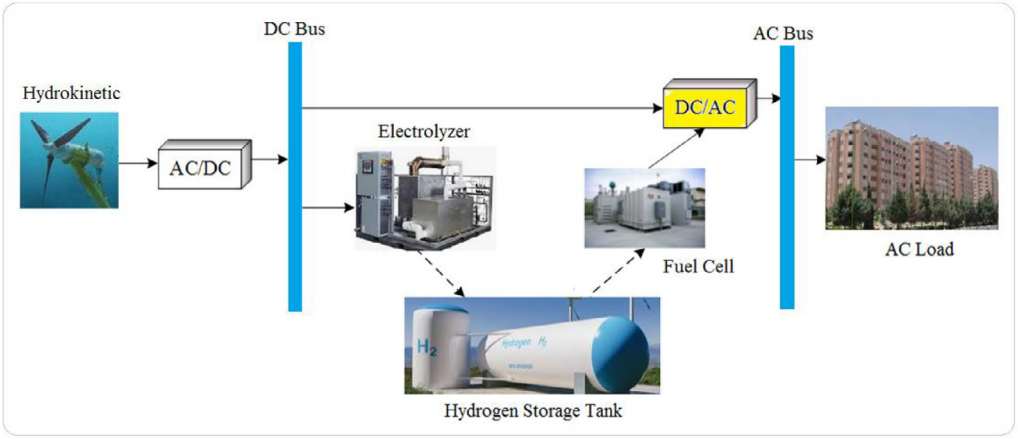

(b)

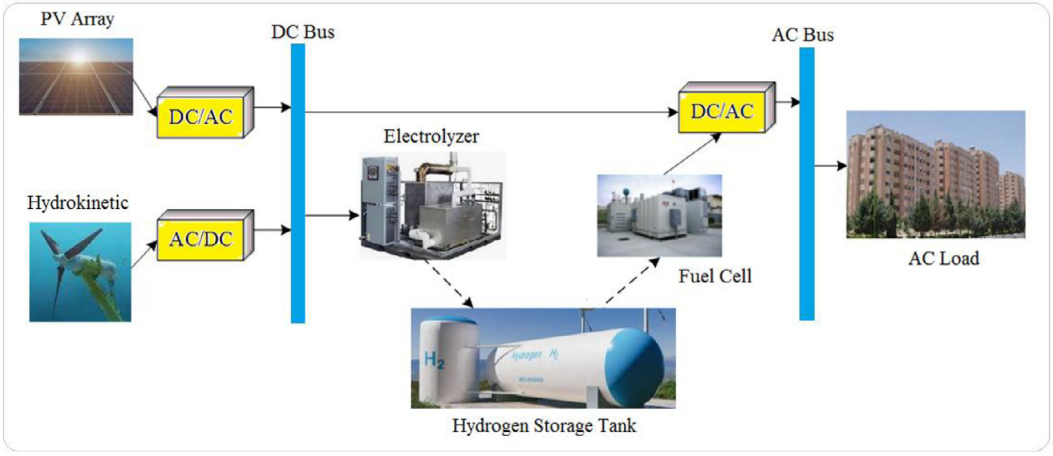

(c)

Fig. 1. Schematic of different configurations of the hybrid energy system.

2019) using desirable optimization method play a very important role in achieving a cost-effective–reliable hybrid energy system (Guo et al., 2018; Liu et al., 2021).

In Table 1, several studies are presented in field of the hybrid systems sizing considering different configurations, storages, economic and technical objectives, and optimization methods. In Heydari and Askarzadeh (2016), a hybrid PV/Biomass system sizing is performed with objective of minimizing the net present cost and considering the loss of power supply as technical constraint via harmony search algorithm (HSA). A modified simulated annealing algorithm is suggested to optimize the hybrid system configurations based on hydrogen using with the goal of life

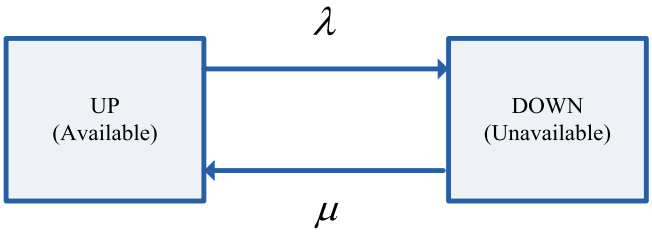

Fig. 2. Two-state Markov model of a component.

cycle cost minimization (Zhang et al., 2018). The size of the hybrid PV/battery/diesel system is determined in Jeyaprabha and Selvakumar (2015), an autonomous area in India country via an artificial intelligence algorithm. In (Kerdphol et al., 2016), a sizing framework is developed with battery storage using particle swarm optimization (PSO) with control of the stand-alone system frequency. In Baghaee et al. (2016), a sizing approach of a PV/Wind system as autonomous is developed to minimize the cost and load un-supplied power with PSO. In Sanajaoba (2019), the autonomous PV/Wind/battery (PV/WT/BA) system is developed considering minimizing the cost of electricity (COE) and satisfying the probability of un-met load using firefly algorithm (FA) in India country. In Hadidian-Moghaddam et al. (2016), a hybrid PV/WT/BA system is designed optimally via grey wolf optimizer (GWO) and aimed at minimizing the energy cost. In Ghorbani et al. (2018), optimization of a PV/WT/BA system is studied using a GA-PSO optimizer with the aim of minimizing the energy cost and considering the LPSP constraint. In Alshammari and Asumadu (2020), the PV/WT/Biomass/BA system sizing is studied with cost minimization and satisfying the LPSP with harmony search, Jaya, and PSO algorithms. In Jahannoosh et al. (2020), the sizing framework of a hybrid PV/Wind/hydrogen system is suggested with the aim of project cost and considering LPSP using hybrid grey wolf optimizer-sine cosine algorithm (HGWO-SCA). In Sadeghi et al. (2020), the optimal size of PV/WT/BA system is found with reliability evaluation using multi-objective PSO. In Maleki et al. (2020), the design of a PV/Fuel cell system is developed to minimize the life cycle cost and with satisfying the LPSP using a harmony search algorithm (HSA). In Sanajaoba and Fernandez (2016), the sizing framework of an autonomous hybrid PV/WT/BA System is developed to minimize the energy cost and considering load supply via cuckoo search (CS) algorithm with outage rate of the WTs. In De and Ganguly (2021), a stand-alone PV/FC system design is proposed for an autonomous cold storage facility considering economic, and environmental factors based on the mixed-integer nonlinear programming (MINLP). In Xu et al. (2021), sizing of autonomous PV/Fuel cell system is evaluated for generation cost minimization via amended water strider algorithm (AWSA) for the autonomous region.

In Abdelshafy et al. (2018), PV/WT/BA sizing as grid-connected is presented with energy cost minimization using MOPSO. In Mayer et al. (2020), the multi-criteria design of an energy system is studied via the GA. The achieved results revealed that the application of the PVs is the logical and economic way for environmental impacts reduction. In Gharibi and Askarzadeh (2019), stand-alone PV/FC/Diesel system design is studied to minimize the energy costs and assessment of the LPSP via a crow search algorithm. In Xu et al. (2020), sizing of PV/WT/Hydro system is developed considering the LPSP and with minimization of the generation cost using the MOPSO in China. In Mohamed et al. (2017), a grid-connected PV/WT energy system is designed to minimize the energy generation cost via PSO considering energy balanced factor. In Naderipour et al. (2021), the sizing of a hybrid WT/HKT/Hydrogen system is developed for minimizing the cost of reliability enhancement and evaluation of shortage load probability via the whale optimizer method. In Arabi-Nowdeh et al. (2021), the design of an autonomous and non-autonomous PV/WT/BA system is solved to minimize the environmental pollutions as well as the cost of system components with an evaluation of the factor of deficit power of the load using spotted hyena optimization (SHO).

Recently, in MiarNaeimi et al. (2021), horse herd Optimization (HHO) algorithm is modeled based on the herding behavior of horses for problems with high-dimensional. The main advantage of the HHO is determination of a position in the initial iterations, optimally. According to the studies conducted in the literature review, sizing of the PV/HKT/FC system is developed via the horse herd optimization (HHO), which performed better than other methods. This method has not been used for sizing the PV/HKT/FC system as far as the authors of the study are concerned.

In this paper, the optimal sizing framework of a hybrid PV/HKT/FC system is formulated considering forced outage rate (FOR) evaluation of the renewable resources to minimize the net present cost of hybrid system (NPCHS) considering environmental information of irradiance, temperature, water flow, and load demand using the HHO algorithm. The purpose of the problem is to apply the HHO to determine the optimal configuration considering the NPCHS and reliability constraint as the probability of load supply (PLS). The effect of changes in the operational probability of photovoltaic and hydrokinetic resources by evaluating the forced outage rate (FOR) (Allan, 2013) due to hardware and structural faults is evaluated and analyzed in sizing of different system configurations. Also, the impact of changes in reliability constraint is evaluated in components sizing, NPCHS, PLS, and also hydrogen energy contribution. Moreover, the superiority of the HHO is compared with well-known PSO, GA, and GWO in system sizing based on the cost and reliability.

The contribution of the research is listed as follows:

- Sizing framework of the autonomous PV/HKT/FC system with hydrogen energy
- Using of horse herd optimization algorithm for solving the hybrid system sizing
- Cost-effective and reliable PV/HKT/FC system with the COE equal to 1.57 $/kWh
- The COE is obtained 1.63 and 1.66 $/kWh with the FOR (8%) for HKTs and PVs
- Superior capability of the HHO compared with PSO, GA, and GWO methods

In Section 2, methodology including understudy region, hybrid system modeling, cost model as the objective function, reliability model as a technical constraint, and optimization algorithm and its implementation are described carefully. In Section 3, the results are described. Finally, in Section 4, the finding are presented.

2. Methodology

The optimal sizing of a hybrid PV/HKT/FC system has been performed to supply the load of an autonomous residential complex. In this section the hybrid system operation and modeling, reliability model of generation resources, cost model, reliability constraint, hybrid energy system management and optimization method and its implementation to solve the sizing problem is described.

2.1. Hybrid system operation and modeling

The hybrid system configurations sizing (see Fig. 1) such as PV/FC, HKT/FC, and PV/HKT/FC systems is performed to find the

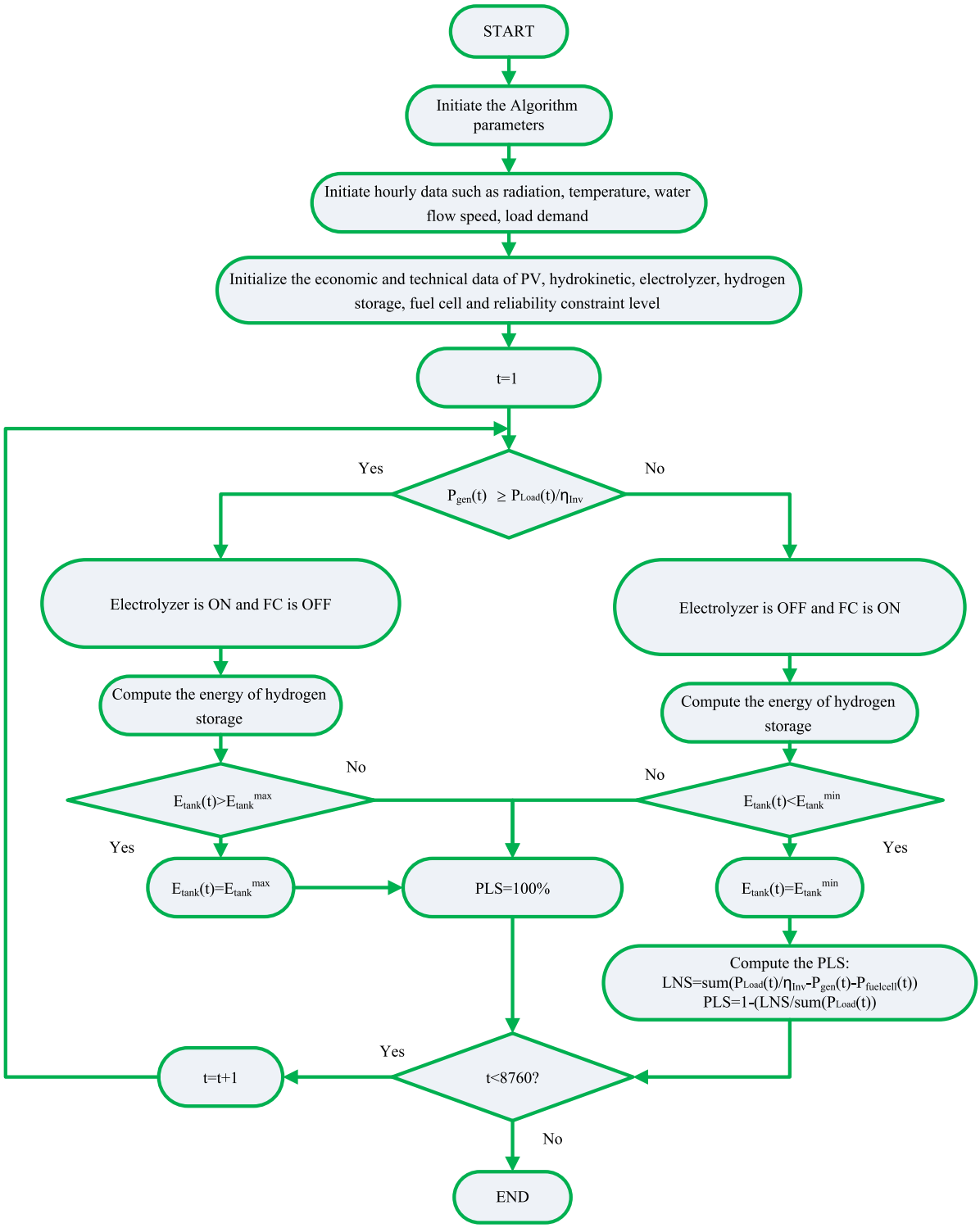

Fig. 3. Flowchart of the LFCCS.

optimal-cost-effective–reliable configuration. The main components of these systems are photovoltaic array, Hydrokinetic system, electrolyzer to generate hydrogen, hydrogen tank storage, fuel cell, and also inverter. The role of the hydrogen storage is to compensate for the fluctuations of generated power and supply the residential complex demand with a desirable reliability level. In Fig. 1, in configuration (a), PV source is the main generation unit of the energy system, in configuration (b) Hydrokinetic is responsible for generating energy in the system and also in configuration (c) PV source with Hydrokinetic generate power by contribution together in the system.

In following the mathematical model of the hybrid system components is presented.

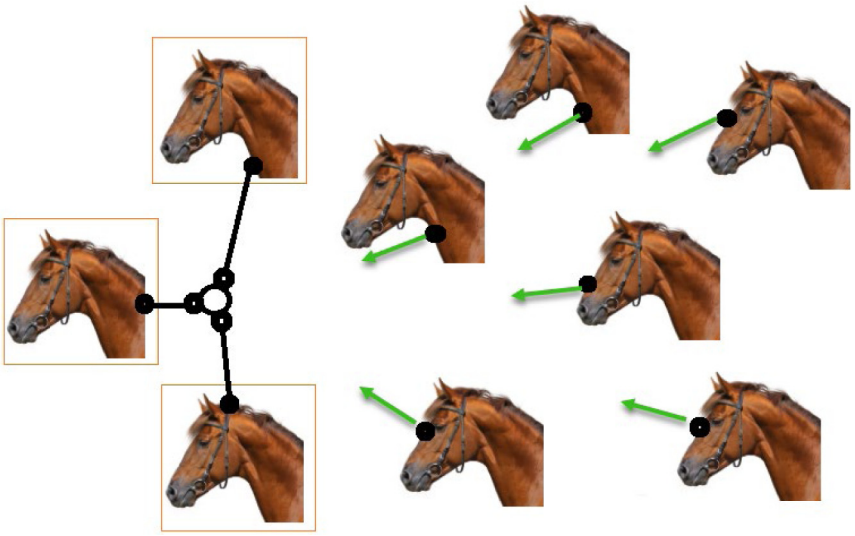

Fig. 4. Imitation behavior of horses (MiarNaeimi et al., 2021).

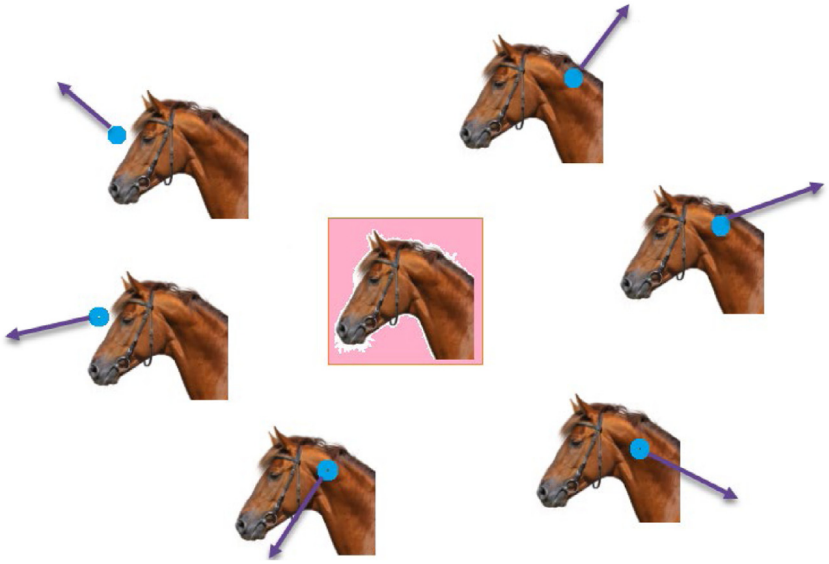

Fig. 5. Defensive behavior of the horses (MiarNaeimi et al., 2021).

a) Main structure: Applying the range of variables and parameters of the algorithm;
b) Initial quantification: Distribution of horses randomly in a practical space;
c) Evaluation of fitness: Evaluate the cost for each horse according to the location and the objective function;
d) Calculating age: determining the age of each horse α, β, γ, δ;
e) Speed application: Considering the speed for each horse according to age;
f) Evaluation of new positions: the position of each horse is updated in search space.
g) Convergence criterion: Go to step c until the convergence criterion and termination of the algorithm are met;

Fig. 6. The HHO pseudo code.

Table 1
Comparison of the proposed hybrid system and methodology with literature.

Ref.	Hybrid system	Cost	Reliability constraint	Forced outage rate (FOR)	Storage	Optimization method	Research gap
(Heydari and Askarzadeh, 2016)	PV/Biomass	✓	✓	×	×	HSA	High cost and without FOR evaluation
(Zhang et al., 2018)	PV/WT/BA	✓	×	×	BA	ACO	Without reliability evaluation and the FOR
(Jeyaprabha and Selvakumar, 2015)	PV/BA/Diesel	✓	✓	×	BA	ANFIS	High cost and without FOR evaluation
(Kerdphol et al., 2016)	PV/BA	✓	×	×	BA	PSO	Premature convergence and without FOR evaluation
(Baghaee et al., 2016)	PV/WT/FC	✓	✓	×	FC	PSO	Without considering the FOR and high sizing cost
(Sanajaoba, 2019)	PV/WT/BA	✓	✓	×	BA	FA	Without FOR evaluation and high designing cost
(Hadidian-Moghaddam et al., 2016)	PV/WT/BA	✓	×	×	BA	GWO	Without reliability evaluation and the FOR
(Ghorbani et al., 2018)	PV/WT/BA	✓	×	×	BA	Genetic-PSO and homer	Without reliability evaluation and the FOR
(Alshammari and Asumadu, 2020)	PV/WT/BA/Biomass	✓	✓	×	BA	PSO	Premature convergence and without FOR evaluation
(Jahannoosh et al., 2020)	PV/WT/FC	✓	✓	×	FC	Grey wolf optimizer-sine cosine algorithm	Without evaluation of the FOR effects
(Bingzhi et al., 2021)	PV/Diesel	✓	×	×	Pumped water	MMRFO	Not studying the reliability and FOR effect on sizing
(Sadeghi et al., 2020)	PV/WT/BA	✓	✓	×	Battery	PSO	Premature convergence and without FOR evaluation
(Maleki et al., 2020)	PV/FC	✓	✓	×	FC	HSA	Not investigating the FOR abd reliability on the system sizing
(Sanajaoba and Fernandez, 2016)	PV/WT/BA	✓	✓	×	BA	CSA	High cost and without FOR investigation
(De and Ganguly, 2021)	PV/FC	✓	✓	×	FC	MINLP	Without reliability/FOR evaluation
(Xu et al., 2021)	PV/FC	✓	✓	×	FC	WSA	Premature convergence and without FOR evaluation
(Abdelshafy et al., 2018)	PV/WT/BA	✓	✓	✓	BA	PSO	Premature convergence and without FOR evaluation
(Mayer et al., 2020)	PV/BA	✓	×	✓	×	GA	Without reliability evaluation and the FOR
(Gharibi and Askarzadeh, 2019)	PV/FC/Diesel	✓	✓	✓	FC	CSA	Without examination of the FOR on system sizing
(Xu et al., 2020)	PV/FC/Hydro	✓	✓	✓	FC	PSO	Without evaluating the FOR effect on sizing
(Mohamed et al., 2017)	PV/WT	✓	×	✓	×	PSO	Without reliability evaluation and the FOR
(Naderipour et al., 2021)	WT/HKT/FC	✓	✓	✓	FC	WOA	Not considering FOR
(Arabi-Nowdeh et al., 2021)	PV/WT/BA	✓	✓	✓	BA	SHO	High cost and without FOR evaluation
This paper	PV/HKT/FC	✓	✓	✓	FC	HHO	Considering cost, reliability, FOR using new horse herd optimization (HHO) algorithm

• *PV model*

The power of the solar array varies according to the module temperature parameters (T_m) and solar radiation (R). Therefore, the amount of production capacity by this type of renewable resources are defined as follows (Jahannoosh et al., 2020; Arabi-Nowdeh et al., 2021):

$$P_{photovoltaic}(R, T_m) = \frac{R}{R_{STC}} \times P_{STC} \times \eta_{IR}\left(R', T'\right) \quad (1)$$

Where, R_{STC} and P_{STC} indicate the radiation intensity and power of the module, respectively, subjected to standard test conditions. Also, η_{IR} represents the efficiency of the PV module, which is defined by

$$\eta_{IR}(R', T') = 1 + k_1 logR' + k_2(logR')^2 + T'\left(k_3 + k_4 logR' + k_5(logR')^2\right) + k_6 T' \quad (2)$$

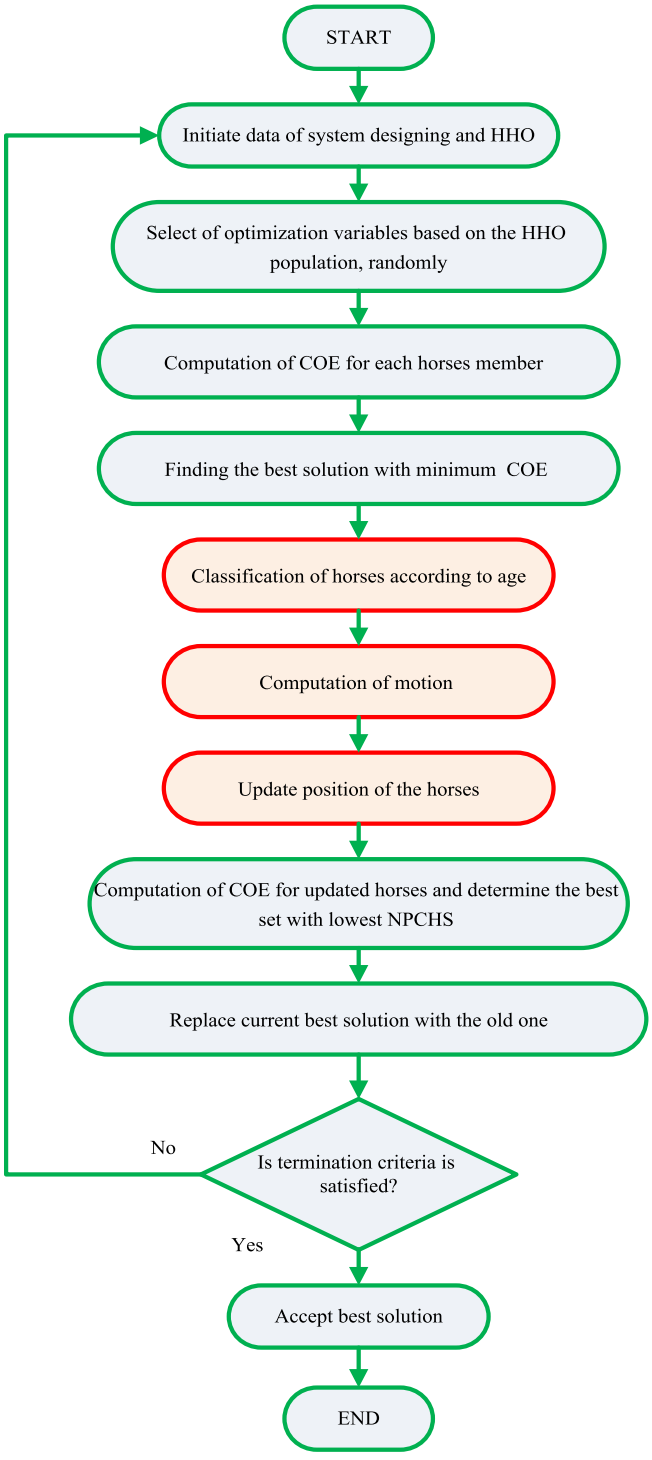

Fig. 7. Flowchart of the HHO implementation in problem solving.

Where, $k_1 - k_6$ refer to the $\eta_{IR}(R', T')$ coefficients that should be determined by model fitting based experimental data investigated in one or more test locations.

Also, R' and T' are also obtained as follows:

$$R' = \frac{R}{R_{STC}} \tag{3}$$

$$T' = T_m - T_{STC} \tag{4}$$

$$T_m = T_a + \frac{[(NOCT - 20^{oc}).R]}{800} \tag{5}$$

• *Hydrokinetic model*

Hydrokinetic turbines are presented to extract the kinetic energy based on flowing water. Hydrokinetic is capable produce power in low water flow with zero environmental affect. The generated power ($P_{hydrokinetic}$) using the hydrokinetic system is defined by Khare (2019) and Kusakana (2014)

$$P_{hydrokinetic} = \begin{cases} P_{hydrokinetic-rtd} \times \left(\frac{WF - WF_{ci}}{WF_{rtd} - WF_{ci}}\right)^3 & ; WF_{ci} \le WF \le WF_{rtd} \\ P_{hydrokinetic-rtd} & ; WF_{rtd} < WF < WF_{co} \\ 0 & \text{Otherwise} \end{cases} \tag{6}$$

$$P_{hydrokinetic-rtd} = 0.5 \times \delta_{wd} \times A_{ta} \times C_P \times \eta_{HKT} \times WF^3 \tag{7}$$

Where, WF indicates velocity of water flow (m/s), WF_{ci} is cut-in water flow (m/s), WF_{co} is cut-in water flow (m/s) and WF_{rtd} is rated water flow (m/s). In this study, WF_{ci}, WF_{rtd} and WF_{co} are selected 0.7, 2.4 and 5 m/s, respectively. $P_{hydrokinetic-rtd}$ is rated power by the HKT unit (kW), δ_{wd} is water density (kg/m^3), A_{ta} is turbine area (v^2), C_P is coefficient related to hydrokinetic performance, and η_{HKT} is efficiency related to hydrokinetic turbine and the generator.

• *Electrolyzer model*

The electrolyzer can generate hydrogen by receiving the electrical power by clean production resources based on the electrolysis process of the water. By delivering hydrogen to the storage tank and storing it under pressure, it is delivered to the fuel cell when needed to generate power. The model of electrolyzer is defined as follows (Jahannoosh et al., 2020; Sanajaoba and Fernandez, 2016):

$$P_{electrolyzer-tank} = P_{gen-electrolyzer} \times \eta_{electrolyzer} \tag{8}$$

Where, $\eta_{\text{electrolyzer}}$ refers to efficiency of electrolyzer, and $P_{gen-\text{electrolyzer}}$ indicates received electrical power from clean production resources.

• *Hydrogen tank model*

The hydrogen is stored subjected to high pressure in the tank. In the event of a load shortage, the hydrogen tank is discharged and delivers hydrogen to the FC to produce power and supply the load shortage. The stored hydrogen energy is defined a follows (Jahannoosh et al., 2020; Sanajaoba and Fernandez, 2016):

$$E_{tank}(t) = E_{tank}(t-1) + [P_{electrolyzer-tank}(t) - P_{tank-fuelcell}(t) \times \eta_{tank}] \times \triangle t \tag{9}$$

Where, $E_{tank}(t-1)$ is hydrogen energy of the tank in time (t-1), $P_{\text{electrolyzer}-\text{tank}}$ refers to the electrolyzer power to tank, $P_{\text{HS to FC}}$ indicates tank power transferred to the fuel cell. Moreover, $E_{\text{tank}}(t) = h_{v,H2} \times Mass_{\text{tank}}(t)$ that $Mass_{\text{tank}}(t)$ is mass of hydrogen (kg) at time t, $h_{v,H2}$ refers to heating value of the hydrogen, and η_{tank} defines the efficiency of the storage tank.

• *Fuel cell model*

The fuel cell produces electricity by receiving hydrogen. In load shortage conditions, the fuel cell can generate power by receiving hydrogen from the storage tank. The fuel cell power is defied by

$$P_{fuelcell-inverter} = P_{tank-fuelcell} \times \eta_{fuelcell} \tag{10}$$

Where, η_{fuelcell} defines the FC efficiency.

• *Inverter model*

The inverter in the end part of the system has the role of converting DC to AC power and delivering it to the demand. The received power by the load from the inverter is defined by

$$P_{inverter-load} = (P_{fuelcell-inverter} + P_{gen-inverter}) \times \eta_{inverter} \tag{11}$$

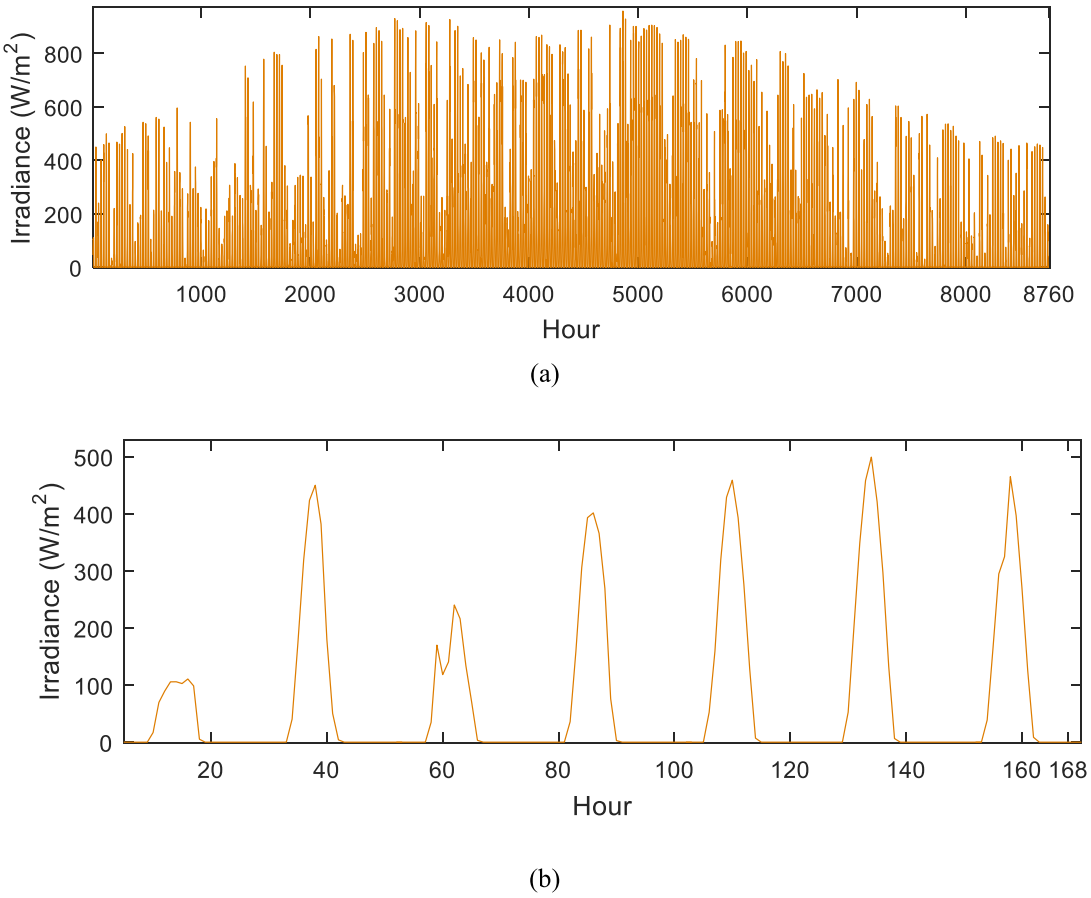

Fig. 8. Hourly solar insolation profile data (a) during a year and (b) during the first 7 d (168 h) of the year.

Where, $\eta_{inverter}$ refers to efficiency of inverter, and $P_{gen-inverter}$ indicates the delivered power by the clean production resources to inverter.

2.2. Reliability model of generation resources

In terms of reliability, no component in a system can have a 100% operational probability and always be successful in operating conditions. In other words, no component is 100% available (in-service) due to unexpected problems as well as failures. Any component must be taken out of service to repair the failure and naturally cannot be available. Therefore, the percentage of time when a component is out of service due to unexpected problems or failures (unscheduled outages) is called the forced outage rate of the component. Fig. 2, shows the two-state Markov model in which, due to failure, a component is transferred from the available state (UP) to the unavailable state (DOWN) and is taken out of service. On the other hand, to transfer it to the available state, it took time to repair the failure, which in this state is out of service (Rajabi-Ghahnavieh and Nowdeh, 2014).

In Fig. 2, λ and μ refer to the failure and repair rate of the component.

The probability of the DOWN or unavailability of the component (FOR) is defined by (Rajabi-Ghahnavieh and Nowdeh, 2014)

$$FOR = \frac{\lambda}{\lambda + \mu} \tag{12}$$

The FOR also in energy system operation base on the hours of the service can be defined by

$$FOR = \frac{HOFO}{HOFO + HOS} \tag{13}$$

Where, $HOFO$ is hours of forced outage and HOS indicates hours of service.

So, based on the defined FOR, the generated power of the PV and HKT units in Eqs. (1) and (6) are rewritten as follows:

$$P_{photovoltaic}(R, T_m) = \frac{R}{R_{STC}} \times P_{STC} \times \eta_{IR}\left(R', T'\right) \times (1 - FOR) \tag{14}$$

$$P_{hydrokinetic} = 0.5 \times \delta_{wd} \times A_{ta} \times C_P \times \eta_{HKT} \times v^3 \times (1 - FOR) \tag{15}$$

2.3. Cost model (objective function)

The cost model for objective function is defined according to capital, operation, and maintenance (O&M) and also replacement costs of components of the hybrid system. The capital cost refers to the cost of purchasing components at the project beginning. The O&M cost is related to the cost that is paid annually during the project lifespan for each component unit or capacity of that component. Replacement cost is also a cost that based on the lifetime of each component should be replaced with another component. In the sizing problem, the system cost should be minimized. So, the cost objective function is defined as follows (Jahannoosh et al., 2020; Sanajaoba and Fernandez, 2016; Mayer et al., 2020; Arabi-Nowdeh et al., 2021):

$$NPCHS = NPC_{I,k} + NPC_{O,k} \times \left(\frac{1}{CRF}\right) + NPC_{R,k} \times R_k \tag{16}$$

$$R_k = \sum_{n=1}^{N} \frac{1}{(1+i)^{L \times n}} \tag{17}$$

$$CRF = \frac{i(1+i)^{TP}}{(1+i)^{TP} - 1} \tag{18}$$

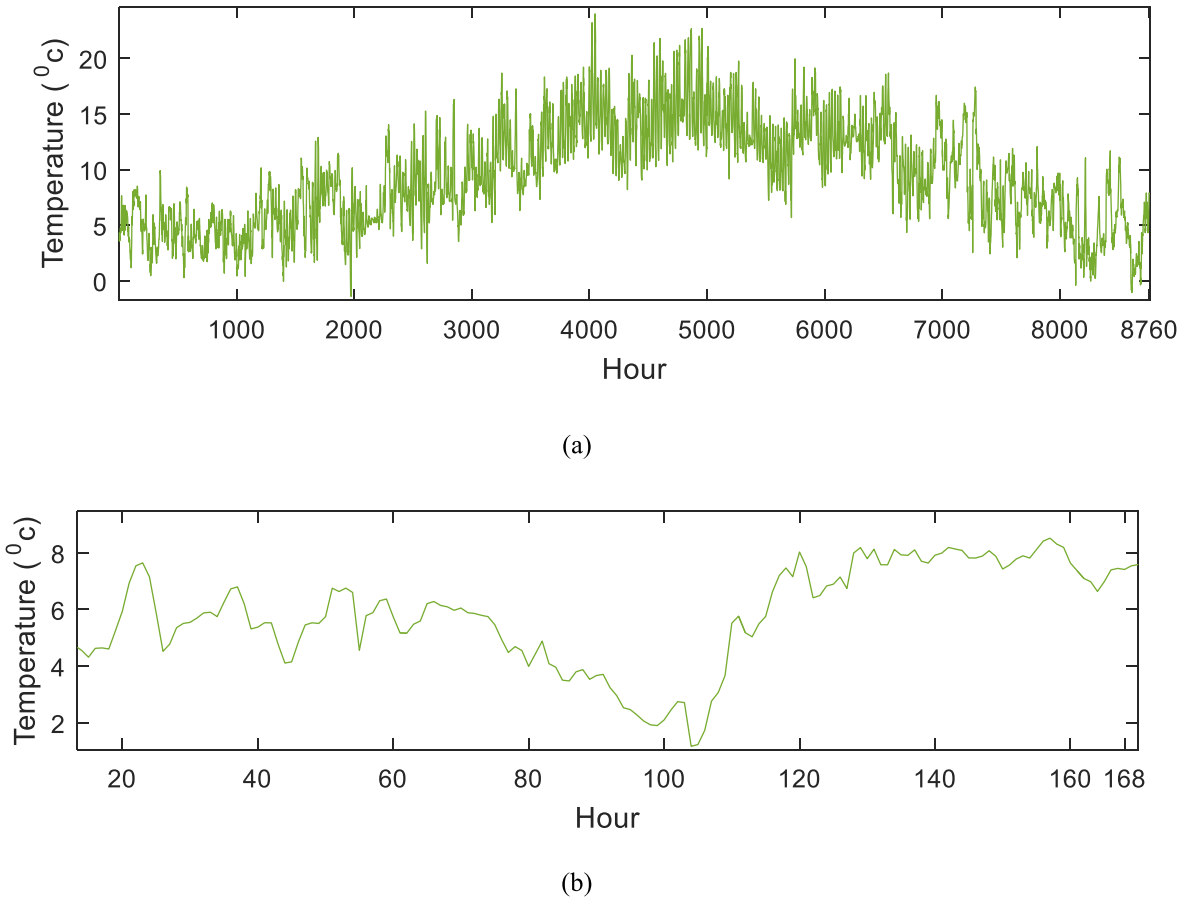

Fig. 9. Hourly temperature profile data (a) during a year and (b) during the first 7 d (168 h) of the year.

Where, $NPC_{I,k}$, $NPC_{O,k}$ and $NPC_{R,k}$ refer to the capital, the O&M and also components replacement costs, respectively. Also, *CRF* is capital recovery factor, R_k is present worth of the single payment, i refers to the rate of real interest (in this study 9%), *N* defines the replacement number for component k, L indicates lifetime of the component k and *T* is project lifetime (20 years).

Also, the cost of energy (COE) is defined as follows to evaluate the economic performance of the hybrid energy system.

$$COE = \frac{NPCHS}{\sum_{t=1}^{T} P_{Load}(t)} \times CRF \tag{19}$$

2.4. Operation constraints

The constraints of lower and upper limit of the components size such as power size of photovoltaic ($P_{photovoltaic}$), Hydrokinetic ($P_{Hydrokinetic}$), electrolyzer ($P_{electrolyzer}$), fuel cell ($P_{fuelcell}$) and inverter ($P_{inverter}$) are presented as follows:

$$P^{min}_{Hydrokinetic} \le P_{Hydrokinetic} \le P^{max}_{Hydrokinetic} \tag{20}$$

$$P^{min}_{photovoltaic} \le P_{photovoltaic} \le P^{max}_{photovoltaic} \tag{21}$$

$$P^{min}_{electrolyzer} \le P_{electrolyzer} \le P^{max}_{electrolyzer} \tag{22}$$

$$P^{min}_{fuelcell} \le P_{fuelcell} \le P^{max}_{fuelcell} \tag{23}$$

$$P^{min}_{inverter} \le P_{inverter} \le P^{max}_{inverter} \tag{24}$$

Also the constraint related to hydrogen mass and tank hydrogen energy is as follows:

$$Mass^{min}_{tank} \le Mass_{tank} \le Mass^{max}_{tank} \tag{25}$$

$$E^{min}_{tank} \le E_{tank} \le E^{max}_{tank} \tag{26}$$

Where, $Mass^{min}_{tank}$ and $Mass^{max}_{tank}$ low and up limits of the hydrogen mass and E^{min}_{tank} and E^{max}_{tank} are low and up limits of the tank hydrogen energy.

2.5. Reliability constraint

An important aspect of hybrid systems sizing is maintaining the reliability of the demand at an acceptable level (Jahannoosh et al., 2020; Sanajaoba and Fernandez, 2016; Mayer et al., 2020; Arabi-Nowdeh et al., 2021). In this study, the probability of load supply (PLS) is defined as a reliability constraint for sizing the autonomous system. The PLS limits are between 0 and 100%. The higher level of the PLS, clear more supply the load with a higher probability. The PLS is defined as follows:

$$LNS(t) = \sum_{t=1}^{T} [P_{Load}(t) / \eta_{inverter} - P_{gen-inverter}(t) - P_{fuelcell-inverter}(t)] \tag{27}$$

$$PLS = 1 - \frac{LNS(t)}{\sum_{t=1}^{T} [P_{Load}(t)]} \tag{28}$$

Where, $LNS(t)$ is load not supplied at time t and *PLS* is reliability constraint an defined by

$$PLS \ge PLS^{min} \tag{29}$$

Where, PLS^{min} refers to the minimum value of the *PLS* constraint.

2.6. System energy management

According to Fig. 3, the load following and cycle charging strategy (LFCCS) is used to manage the energy in the hybrid

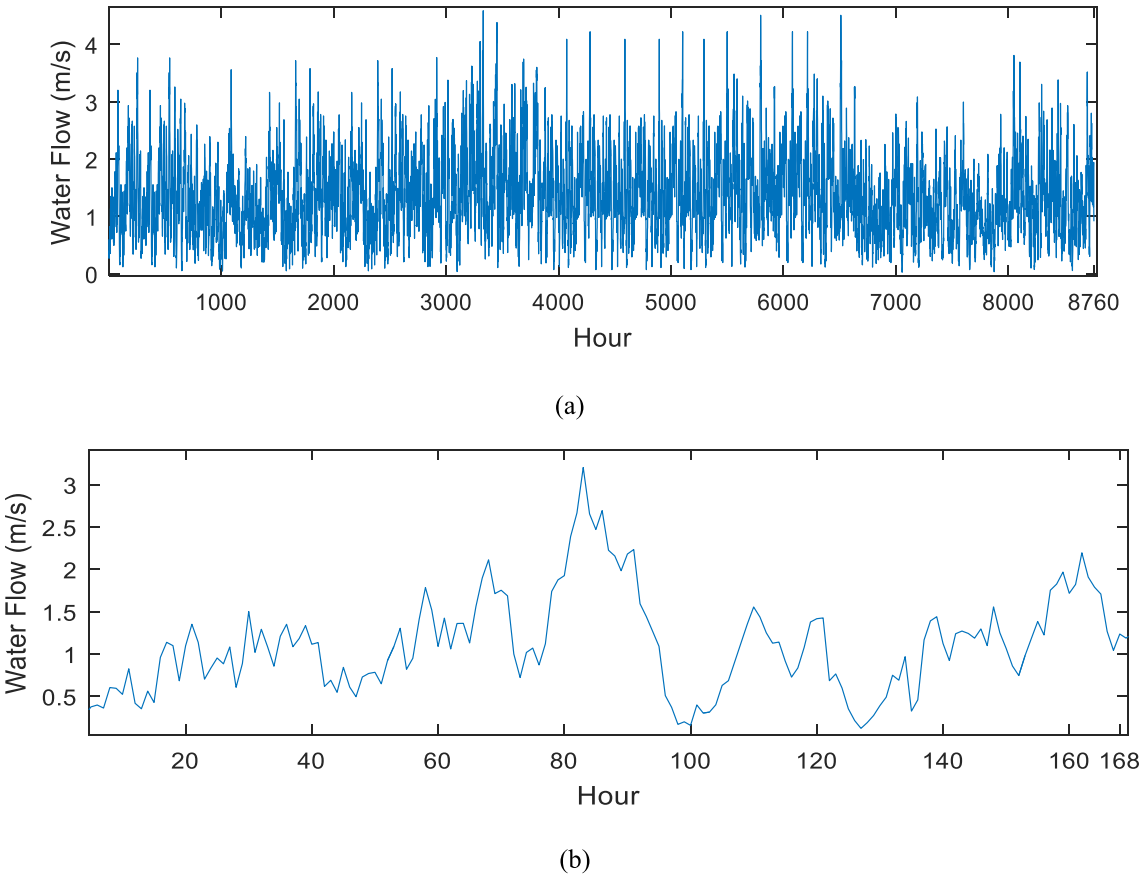

Fig. 10. Hourly water flow data (a) during a year and (b) during the first 7 d (168 h) of the year.

system sizing. Using the LFCCS causes reliability enhancement with the management of the hydrogen storage energy in extra and shortage conditions of the load demand. In the strategy used, the priority is to supply the load at all times. If the produced power in the system is greater than the load, extra power is injected into the electrolyzer for hydrogen generation and in this condition, the fuel cell is off and the probability of load supply (PLS) is 100%.

If the produced power by the system is not able to fully meet the load ($P_{Hydrokinetic}(t) + P_{photovoltaic}(t) < \frac{P_{Load}(t)}{\eta_{Inv}}$), in this case, the lack of load capacity is compensated by the storage system by delivering hydrogen to the fuel cell and producing the middle power. If the storage system is not able to fully compensate the load, in this case, some load will be disconnected and the PLS should be computed.

2.7. Overview HHO and implementation

The horse herd optimization (HHO) is modeled by the life behavior of horses. In modeling the HHO, different patterns in the life of horses at different ages including grazing (G), hierarchy (H), sociability (S), imitation (I), defense mechanism (D), and roam (R) are considered (MiarNaeimi et al., 2021).

The movement of the horses in each repetition is presented by (MiarNaeimi et al., 2021)

$$X_m^{Iter,AGE} = \overrightarrow{V}_m^{Iter,AGE} + X_m^{(Iter-1),AGE}, \quad AGE = \alpha,\ \beta,\ \gamma,\ \delta \tag{30}$$

Where, $X_m^{Iter,AGE}$ is position of the horse m, AGE represents the age range of the horse, Iter is the present iteration, and $\overrightarrow{V}_m^{Iter,AGE}$ is velocity vector of the horse. δ is age range of horses among zero and 5 years, γ related to horses 5 to 10 years, β indicates horses between 10 to 15 years and α represents horses older than 15 years. In the matrix of responses considered in the HHO algorithm, the initial 10% of the matrix represents the α horse, the next 20% refers to the β horses, also the γ and δ horses include the remaining 30% and 40% of the horses (MiarNaeimi et al., 2021).

The vector related to the movement of horses in different age groups in each iteration of the algorithm is defined as follows (MiarNaeimi et al., 2021).

$$\overrightarrow{V}_m^{Iter,\alpha} = \overrightarrow{G}_m^{Iter,\alpha} + \overrightarrow{D}_m^{Iter,\alpha} \tag{31}$$

$$\overrightarrow{V}_m^{Iter,\beta} = \overrightarrow{G}_m^{Iter,\beta} + \overrightarrow{H}_m^{Iter,\beta} + \overrightarrow{S}_m^{Iter,\beta} + \overrightarrow{D}_m^{Iter,\beta} \tag{32}$$

$$\overrightarrow{V}_m^{Iter,\gamma} = \overrightarrow{G}_m^{Iter,\gamma} + \overrightarrow{H}_m^{Iter,\gamma} + \overrightarrow{S}_m^{Iter,\gamma} + \overrightarrow{I}_m^{Iter,\gamma} + \overrightarrow{D}_m^{Iter,\gamma} + \overrightarrow{R}_m^{Iter,\gamma} \tag{33}$$

$$\overrightarrow{V}_m^{Iter,\delta} = \overrightarrow{G}_m^{Iter,\delta} + \overrightarrow{I}_m^{Iter,\delta} + \overrightarrow{R}_m^{Iter,\delta} \tag{34}$$

The behavioral patterns of horses' lives are described below.

• *Grazing (G)*

The grazing area around each horse is modeled with a factor of g. The horses graze without age restrictions for the rest of their lives. The horse grazing behavior is defined as follows (MiarNaeimi et al., 2021).

$$\overrightarrow{G}_m^{Iter,AGE} = g_{Iter}\left(\breve{u} + p\breve{l}\right)\left[X_m^{(Iter-1)}\right], \quad AGE = \alpha,\ \beta,\ \gamma,\ \delta \tag{35}$$

$$g_m^{Iter,AGE} = g_m^{(Iter-1),AGE} \times w_g \tag{36}$$

Where, $\overrightarrow{G}_m^{Iter,AGE}$ represents the movement parameter of the horse i, which has a decreasing trend in each repetition linearly proportional to ω_g. $\breve{l}$ and $\breve{u}$ is lower and upper ranges are the grazing space (between 0.95 and 1.05), and p represent a number

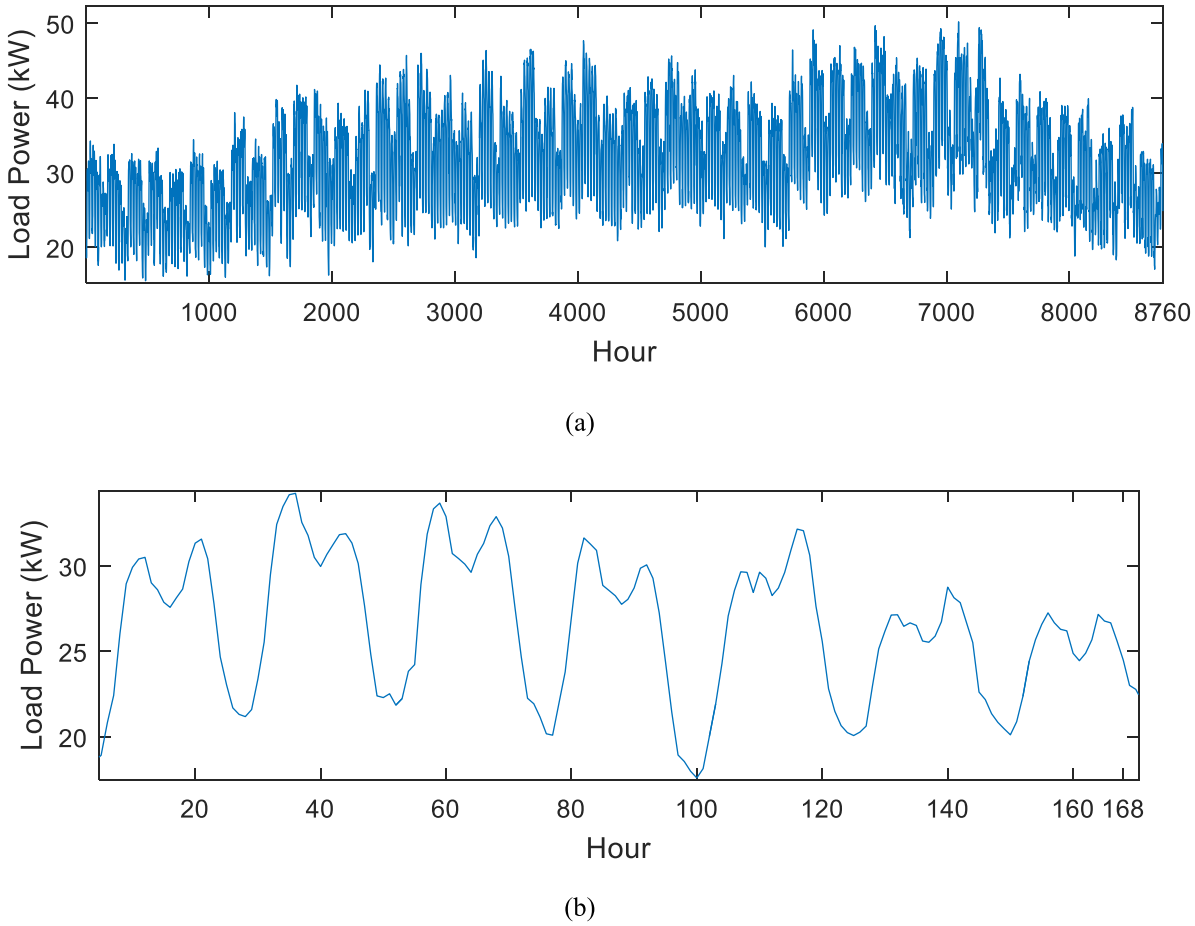

Fig. 11. Hourly load demand data (a) during a year and (b) during the first 7 d (168 h) of the year.

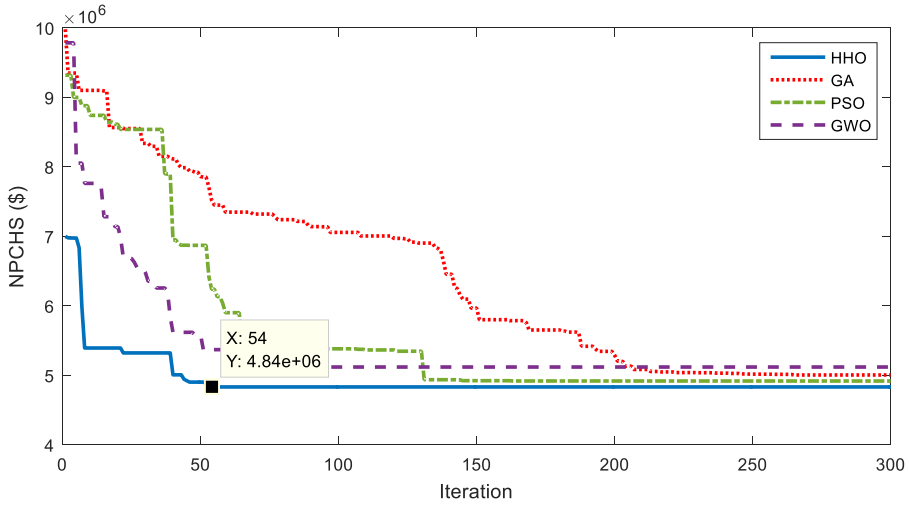

Fig. 12. Convergence process of different algorithms for optimal hybrid PV/HKT/FC configuration for sizing with PLS^{min} = 95%.

among 0 and 1, randomly. The value of g is also considered for all horses without age limit of 1.5 (MiarNaeimi et al., 2021).

• *Hierarchy (H)*

The horses have a leader who is mostly in charge of humans. A stallion or a mare is also liable for leading a herd of wild horses. The coefficient h in the HHO algorithm indicates the interest of a herd of horses to accompany the most powerful and experienced horse (among horses β and γ). This hierarchical behavior is presented as follows (MiarNaeimi et al., 2021):

$$\overrightarrow{H}_m^{Iter,AGE} = h_m^{Iter,AGE}\left[X_*^{(Iter-1)} - X_m^{(Iter-1)}\right], \quad AGE = \alpha,\ \beta\ and\ \gamma \tag{37}$$

$$h_m^{Iter,AGE} = h_m^{(Iter-1),AGE} \times w_h \tag{38}$$

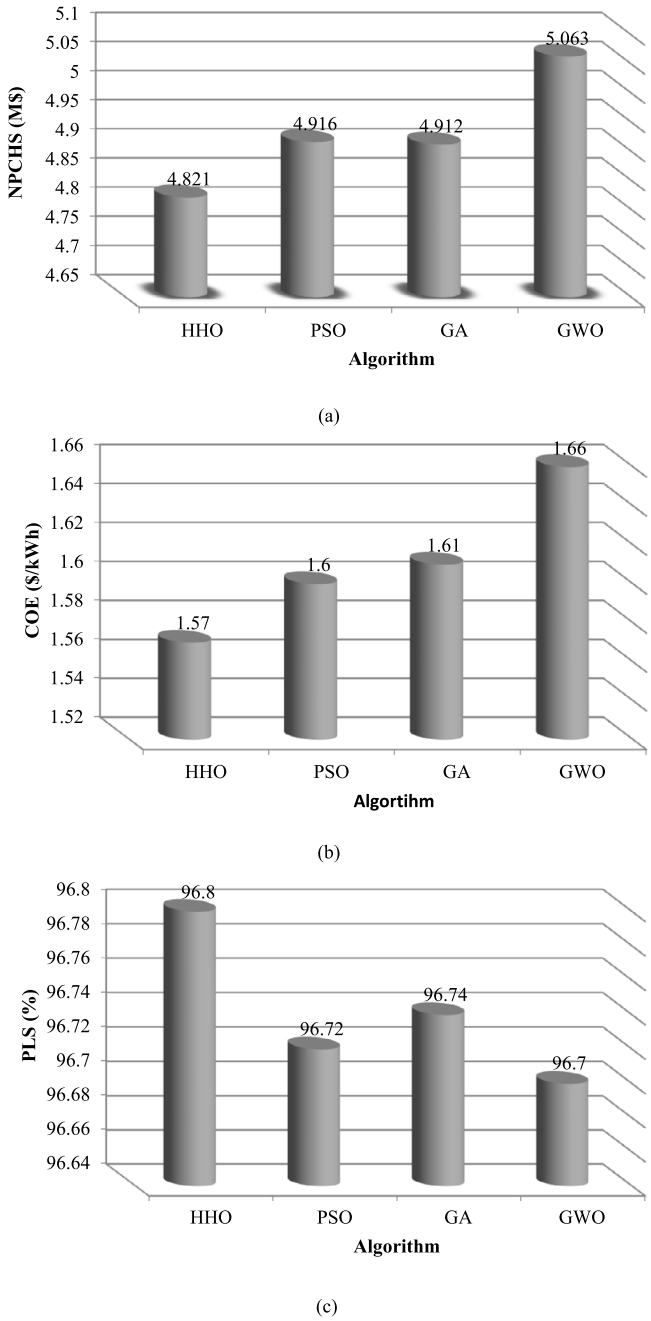

Fig. 13. (a) NPCHS, (b) COE and (c) PLS for sizing of optimal PV/HKT/FC configuration with different methods and with PLS^{min} = 95%.

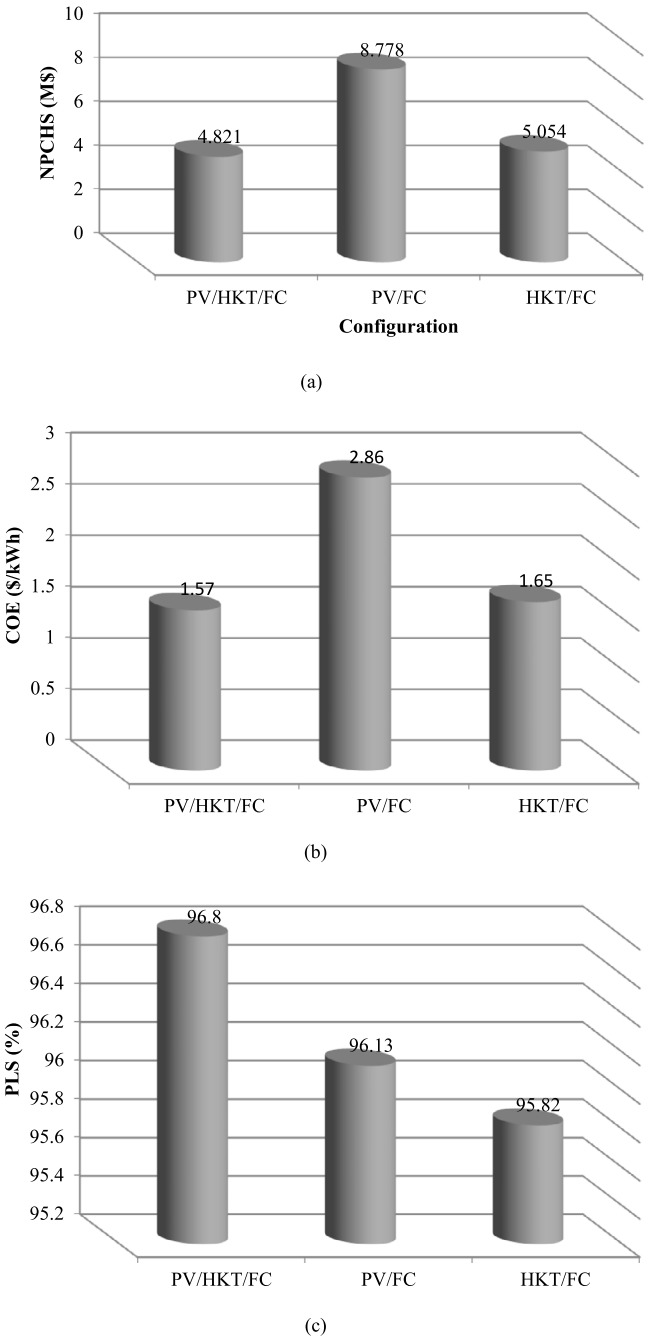

Fig. 14. (a) NPCHS, (b) COE and (c) PLS for sizing of different configurations using HHO and with PLS^{min} = 95%.

Where, $\overrightarrow{H}_m^{Iter,AGE}$ refers to the effect of the best position of the horse in terms of speed and $X_*^{(Iter-1)}$ indicates the position of the best horse.

• *Sociability (S)*

The horses live socially, which is due to their safety and survival. Their social behavior is expressed by a movement towards the position of the other horses and is represented by the parameter s. Most horses β and γ are more interested in herd life, which is modeled as follows (MiarNaeimi et al., 2021).

$$\overrightarrow{S}_m^{Iter,AGE} = s_m^{Iter,AGE}\left[\left(\frac{1}{N}\sum_{j=1}^{N} X_j^{(Iter-1)}\right) - X_m^{(Iter-1)}\right], \quad AGE = \beta \text{ and } \gamma \tag{39}$$

$$s_m^{Iter,AGE} = s_m^{(Iter-1),AGE} \times w_s \tag{40}$$

Where, $\overrightarrow{S}_m^{Iter,AGE}$ represents movement vector of horse i as socially, $S_m^{Iter,AGE}$ is direction of movement of the horse i towards the herd in the Iter iteration. The $S_m^{Iter,AGE}$ in each iteration, considering the coefficient ω_s, there is a decreasing trend. *N* indicates the total horses number and AGE is the age range of each horse.

• *Imitation*

Imitation behavior of the horses is shown in Fig. 4. The horses imitate their behaviors, such as finding a suitable pasture. The imitation of horses is considered based on a factor of i. The imitation behavior is more related to young horses (MiarNaeimi

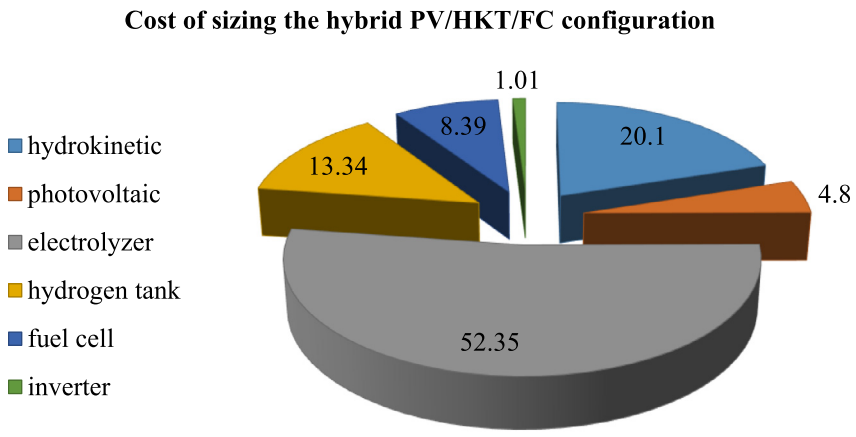

Fig. 15. The cost contribution of the optimal PV/HKT/FC configuration components using HHO and with PLS^{min} = 95%.

et al., 2021).

$$\overrightarrow{I}_m^{Iter,AGE} = i_m^{Iter,AGE}\left[\left(\frac{1}{pN}\sum_{j=1}^{pN}\hat{X}_j^{(Iter-1)}\right) - X_m^{(Iter-1)}\right], \quad AGE = \gamma \tag{41}$$

$$i_m^{Iter,AGE} = i_m^{(Iter-1),AGE} \times w_i \tag{42}$$

Where, $\overrightarrow{I}_m^{Iter,AGE}$ represents the vector of movement of the horse i towards a horse with locations $\hat{x}$, pN is number of horses with the best places (10% of the horses).

• *Defense mechanism (D)*

The horses' defensive behavior is in the form of running away from the horses and buckling, which is considered as a non-optimal response (Fig. 5). Horses' defensive behavior is expressed by a factor of d. The horses' defensive behavior is presented as a negative coefficient in the following model to keep the horses away from undesirable solutions (MiarNaeimi et al., 2021).

$$\overrightarrow{D}_m^{Iter,AGE} = -d_m^{Iter,AGE}\left[\left(\frac{1}{qN}\sum_{j=1}^{qN}\hat{X}_j^{(Iter-1)}\right) - X_m^{(Iter-1)}\right], \quad AGE = \alpha,\ \beta,\ \gamma \tag{43}$$

$$d_m^{Iter,AGE} = d_m^{(Iter-1),AGE} \times w_d \tag{44}$$

Where, $\overrightarrow{D}_m^{Iter,AGE}$ is escape vector of the horse i of the horses mean with the worst places, qN represents the horses number with the worst places (20% of the total horses) and ω_d is the reduction coefficient per iteration.

• *Roaming*

In nature, horses search and roam from pasture to pasture for food. The roaming behavior is a random motion and is defined by the coefficient r. This behavior is more related to young horses and this behavior is eliminated with age. Wandering behavior is defined as follows:

$$\overrightarrow{R}_m^{Iter,AGE} = r_m^{Iter,AGE} pX_m^{(Iter-1)}, \quad AGE = \gamma,\ \delta \tag{45}$$

$$r_m^{Iter,AGE} = r_m^{(Iter-1),AGE} \times w_r \tag{46}$$

Where, $\overrightarrow{R}_m^{Iter,AGE}$ is the horse velocity vector i for escaping local minima, randomly and ω_r is the reduction coefficient per iteration.

The HHO pseudo code is demonstrated in Fig. 6.

The HHO flowchart for the system sizing is demonstrated in Fig. 7. The steps of the sizing solving are as follows.

Step (1) Insert the parameters of system data as radiation, temperature, and water flow data during a year, cost and size data of components, and also the HHO parameters include population (horses) and maximum iteration number.

Step (2) Considering the optimization variables set for the HHO population, randomly. In Section 2.4, the range of variables is presented.

Step (3) The COE in Eq. (19), is calculated for each variables set considered for the HHO population.

Step (4) Determine the best horse with minimum COE value satisfying the constraints.

Step (5) Update the HHO population and determination of the variables set again, randomly.

Step (6) Compute the COE for the new choices set variables in Step 5.

Step (7) Determine the best set variable in view of lower COE at step 7, and replace it if it is lower.

Step (8) Investigation of convergence criteria. If the criteria (perform the maximum iteration and achieving to lowest HSNPC) are met, go to step 9; otherwise, go to step 5.

Step (9) Save the optimal size of the system components and stop the HHO.

3. Results and discussion

3.1. Sizing data

In this section, simulation results of the sizing framework for autonomous hybrid PV/HKT/FC system are given considering FOR using the HHO Algorithm. The sizing framework is implemented to supply the autonomous residential complex. The environmental information includes annual radiation, temperature, and water flow are depicted in Figs. 8–10 and derived from (Naderipour et al., 2021). The annual total load demand is equal to 277.78 MWh and its annual profile is demonstrated in Fig. 11. Moreover, data of system components size and cost are presented in Table 2.

In this study, the capability of the HHO is compared with the PSO, GA, and GWO in the hybrid system sizing. The number of the HHO populations, maximum iterations, and repetitions is considered as 50, 300, and 20, respectively using the trial and error approach and authors' experiences. The optimization variables are found optimally via the HHO, PSO, GA, and GWO for configurations of the hybrid system (Fig. 1). The lower and upper values of the optimization variables are selected 0 and

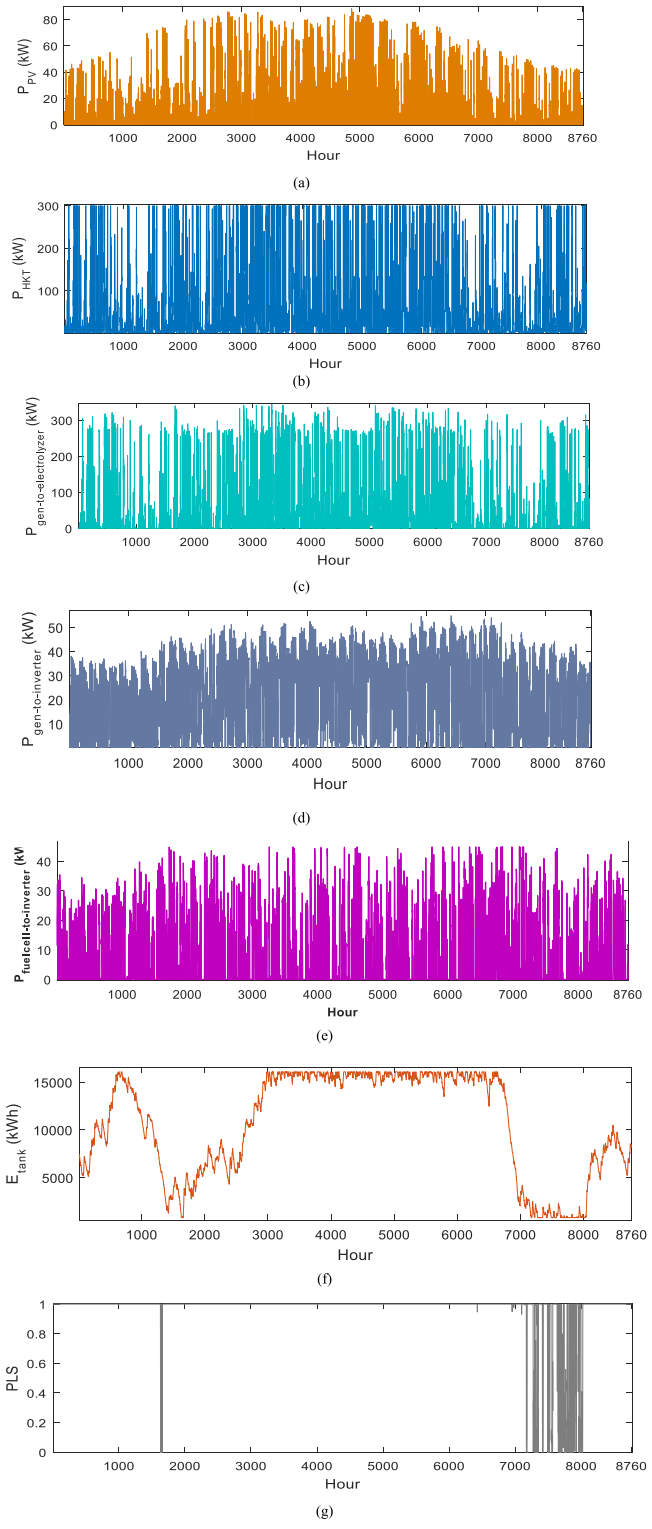

Fig. 16. Power contribution of the hybrid PV/HKT/FC configuration (a) photovoltaic (b) hydrokinetic (c) hybrid power to electrolyzer (d) hybrid power to inverter (e) fuel cell power (f) hydrogen storage energy (g) PLS variations during a year.

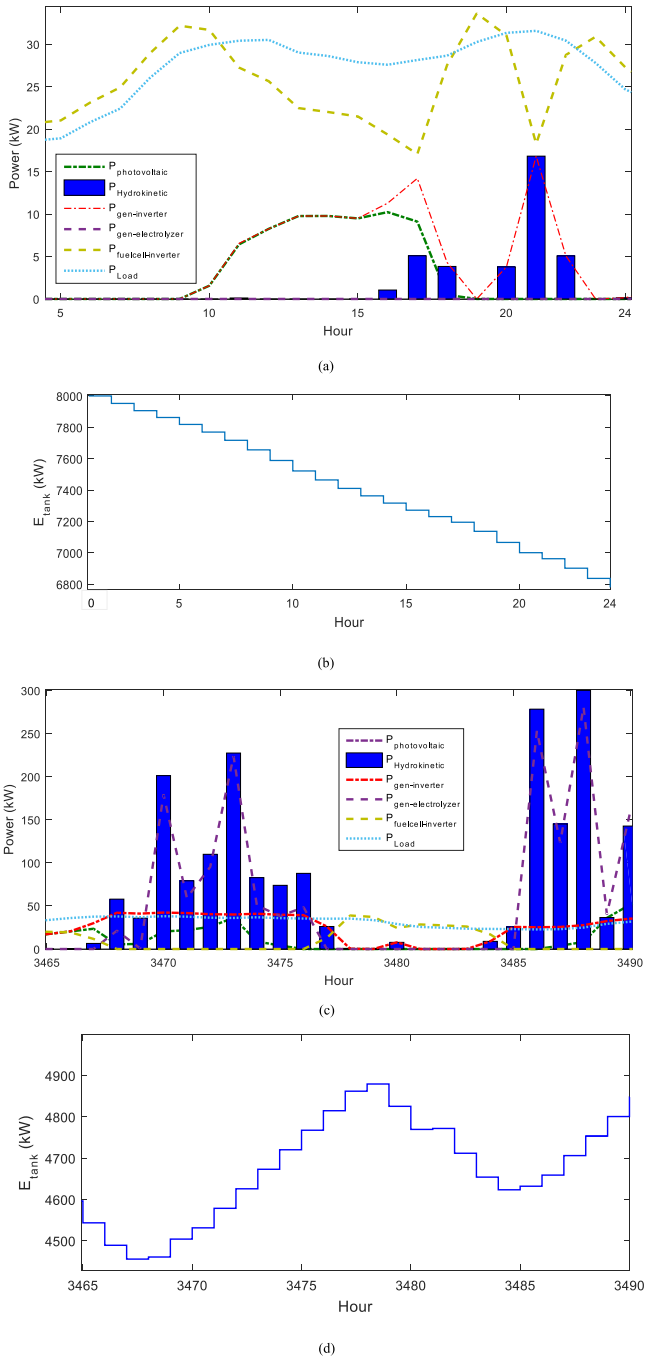

Fig. 17. (a) Power contribution of the hybrid PV/HKT/FC system components (a) during first 24 h (b) tank hydrogen storage energy during first 24 h (c) during hours 3465 to 3490 (d) tank hydrogen storage energy during hours 3465 to 3490.

1000, respectively. In this section results of sizing the configurations of the hybrid system are presented with aim of the COE minimization and satisfying the PLSmin = 95% using HHO, PSO, GA, and GWO methods. The effect of PLSmin variations also is investigated on the sizing problem, COE, and also reliability of the load. Moreover, the effect of considering FOR variations is studied on the sizing problem and in this condition examines which configuration of the autonomous system is more cost-effective and with higher reliability.

3.2. Sizing of different hybrid system configurations

In this section, optimal sizing results of different configuration of an autonomous hybrid system such as PV/FC, HKT/FC, and PV/HKT/FC systems are presented with minimizing the NPCHS and also the COE and satisfying the PLSmin = 95% using the

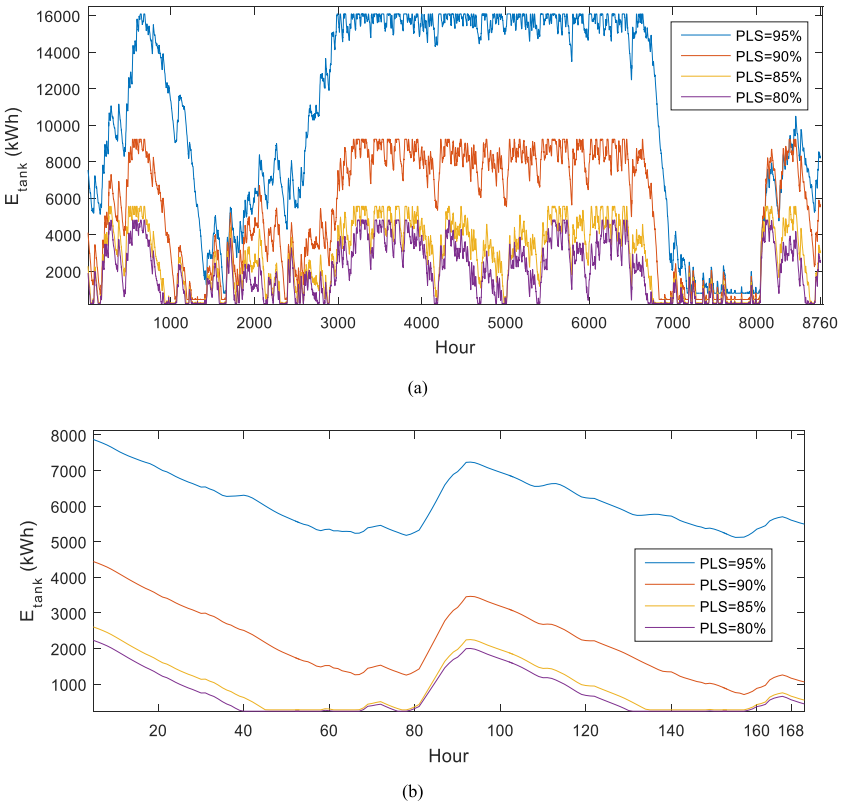

Fig. 18. Hydrogen storage energy in PV/HKT/FC system (a) during a year and (b) during the first 7 d (168 h) of the year considering different PLS^{min}.

HHO Algorithm. In this comparative study, the more effective configuration of the hybrid system in view of cost and reliability is determined. Also, the superiority of the sizing framework based on the HHO is evaluated with PSO, GA, and GWO methods. The results of sizing the different configurations of the hybrid system using HHO, PSO, GA, and GWO methods considering PLSmin = 95%. As it is clear in Table 3, the PV/HKT/FC configuration has the minimum COE and higher PLS (optimal configuration) in sizing problem-solving in different optimization methods in comparison with the other system contributions such as hybrid PV/FC, HKT/FC systems. The convergence process of the HHO, PSO, GA, and GWO for PV/HKT/FC configuration sizing with PLSmin = 95% is depicted in Fig. 12. In Fig. 12, the optimization performance of the HHO algorithm in PV/HKT/FC configuration sizing is showed compared with PSO, GA, and GWO methods. As shown in Fig. 12, the HHO is obtained lowest cost (NPCHS) with lower convergence tolerance. So the better performance of the HHO is proved compared with the other methods.

The results of cost and reliability of different configurations sizing and optimization methods with PLSmin = 95% considering statistic analysis are presented in Table 3. Also, performance of the algorithms under multiple solutions (NPCHS values) in sizing of hybrid PV/HKT/FC system with PLS^{min} = 95% is presented in Table 4. Moreover, results of sizing with different configurations and optimization methods with PLSmin = 95% are presented in Table 5. The NPCHS is obtained 4.821 M$, 4.916 M$, 4.912 M$, and 5.063 M$ using the HHO, PSO, GA, and GWO methods, respectively in PV/HKT/FC configuration sizing. The COE is obtained 1.57 $/kWh, 1.60 $/kWh, 1.61 $/kWh, and 1.66 $/kWh using the HHO, PSO, GA, and GWO methods, respectively. Also, the PLS is achieved 96.80%, 96.72%, 96.74%, and 96.70% using the HHO, PSO, GA, and GWO methods, respectively in PV/HKT/FC configuration sizing. the results showed that the HHO is superior compared with PSO, GA, and GWO methods in achieving to lowest NPCHS and highest PLS in hybrid PV/HKT/FC configuration sizing. Moreover, the superiority of the HHO compared with the other algorithm in a statistic analysis in Table 3, is cleared with fewer values of Best, Mean, Worst, and standard deviation values. Also, this superiority is obtained in sizing of hybrid PV/FC, HKT/FC configurations for the HHO algorithm compared with PSO, GA, and GWO methods. Moreover, according to Table 3, the results cleared the hybrid PV/HKT/FC configuration is the best option with the lowest cost and more reliability to supply the autonomous residential complex in comparison with the other system configurations. The COE is obtained 1.57 $/kWh, 2.86 $/kWh, and 1.65 $/kWh in sizing of the PV/HKT/FC, PV/FC, and HKT/FC configurations, respectively using the HHO algorithm. Also, the PLS is given 96.80%, 96.13%, and 95.82% in sizing of the PV/HKT/FC, PV/FC, and HKT/FC configurations, respectively using the HHO.

The NPCHS, COE, and PLS in sizing of the optimal configuration as PV/HKT/FC system considering PLSmin = 95% is depicted in Fig. 13. As it is clear in this figure, the HHO is achieved lower NPCHS (sizing cost) and also More PLS (better reliability) compared with the other algorithms. Also, Fig. 14, showed that the PV/HKT/FC configuration is cost-effective–reliable option to meet the autonomous residential complex demand with minimum cost and highest reliability level compared with the other system configurations. The cost contribution of the optimal PV/HKT/FC configuration components using HHO and with PLSmin = 95% is demonstrated in Fig. 15. As it is obvious, the more value of the NPCHS is related to electrolyzer (52.35%) and less value of this cost is belongs to inverter devices (1.01%). Also after the electrolyzer system the hydrokinetic, hydrogen tank, fuel cell and photovoltaic devices are contributed with 20.10%, 13.34%, 8.39%, and 4.80% of the NPCHS, respectively.

The power contribution of the hybrid PV/HKT/FC system components with PLSmin = 95% using HHO during a year includes

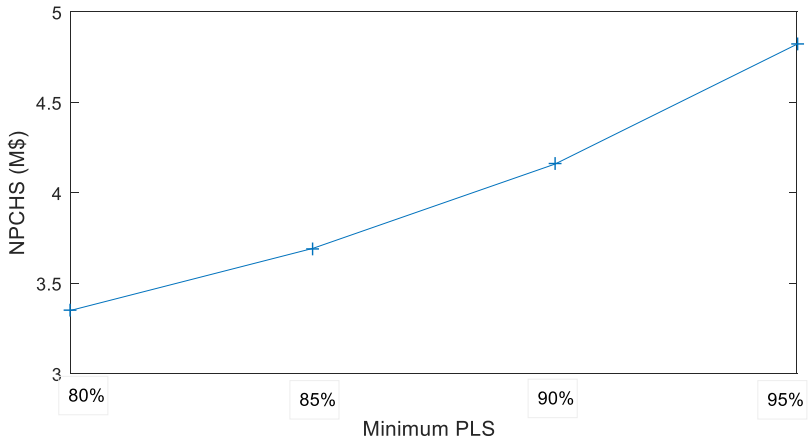

(a)

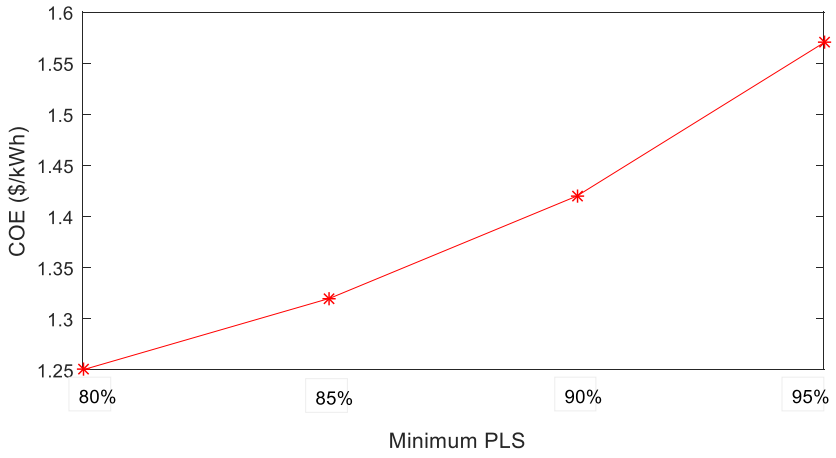

(b)

Fig. 19. (a) The NPCHS and (b) COE versus PLS^{min} variations in hybrid PV/HKT/FC system sizing.

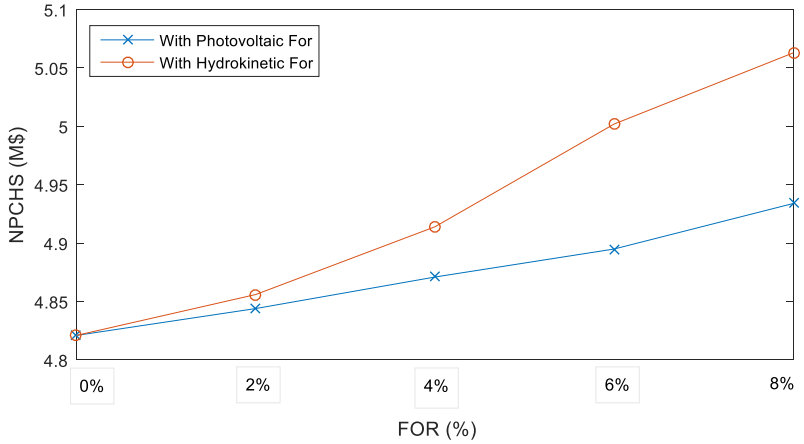

Fig. 20. The NPCHS variations with different FOR_{PV} in different configurations with PLS^{min} = 95% and HHO.

produced power by photovoltaic, hydrokinetic, fuel cell, injected power to electrolyzer by the hybrid system, injected power from hybrid system to the inverter, and hydrogen storage energy is showed in Fig. 16. The hydrogen storage system has created an economic-reliable power supply system by managing the hydrogen energy between power clean production resources (photovoltaic and hydrokinetic) with the load. In other words, the hybrid system based on hydrogen storage creates a continuous supply of the load demand so that the power shortage is compensated based on the injection of hydrogen into the fuel cell and the generation of power by it. Variations of PLS during a year are also depicted in Fig. 16. As shown in this figure, in hours of 7000 to 8000, the reliability of the PV/HKT/FC configuration is decreased due to the reduction of clean production resources and reducing

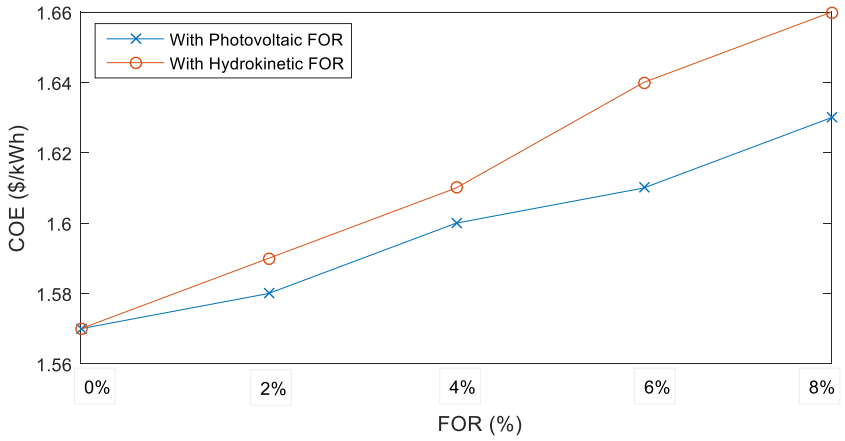

Fig. 21. The COE variations with different FOR_{PV} in different configurations with PLS^{min} = 95% and HHO.

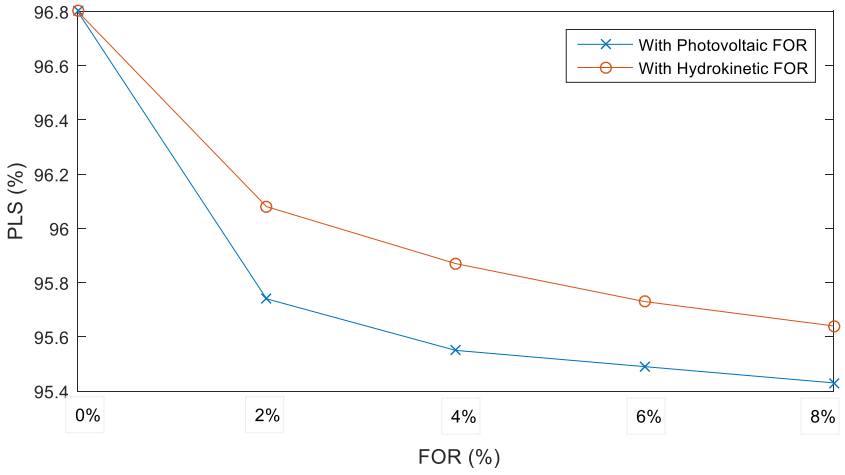

Fig. 22. The PLS variations with different FOR_{PV} in different configurations with PLS^{min} = 95% and HHO.

the hydrogen storage level. Moreover, the power contributions of the hybrid PV/HKT/FC system components during a first day and also hours 3465 to 3490 are demonstrated in Fig. 17, that this figure indicates the overlap of clean production resources, injected power to the electrolyzer from the hybrid system, transferred power to the inverter from the hybrid system, and also the hydrogen storage tank energy to meet the load with high reliability.

3.3. Effect of PLS^{min} variations

The effect of PLSmin variations is evaluated on the sizing of the hybrid PV/HKT/FC configuration using the HHO. The PLSmin is defined as a technical reliability constraint to determine the load supply level by the hybrid system. The system sizing, cost, and reliability of the load supplied is affected by this constraint. So, due to the importance of this constraint, the PLSmin variations effect is investigated on the hybrid PV/HKT/FC sizing. The rated PLSmin is considered 95% in the base study according to Table 2 and in this section, the effect of considering PLSmin = 95, 90, 85 and 80% is evaluated on the sizing of the hybrid PV/HKT/FC configuration. The results in Table 6, cleared that with decreasing the PLSmin (less supply of the load), the NPCHS and COE are reduced due to reduction of resources generation and also decreasing the hydrogen storage level (see Fig. 18) but the PLS is reduced or the system reliability is weakened. In Fig. 18, the hydrogen storage energy in PV/HKT/FC system during a year and also during the first week (168 h) of the year with different PLSmin is presented. As shown as in this figure, with decreasing the PLSmin, the hydrogen energy level is reduced and vice versa. Moreover, the NPCHS and PLS, NPCHS and COE and COE and Masstank of the hybrid PV/HKT/FC system with different PLSmin is depicted in Fig. 19. As it is obvious, the NPCHS and COE are increased with increasing the PLSmin values (reliability improvement).

3.4. Effect of considering forced outage rate (FOR)

The effect of FOR variations is presented in Table 7 on the hybrid PV/HKT/FC system sizing via the HHO. In the base study, the operational probability of the hybrid system is considered 100% without FOR. In this study, the effect of FOR equal to 2, 4, 6 and 8% for photovoltaic and hydrokinetic is evaluated on the hybrid PV/HKT/FC system sizing. As a result, these clean production resources are available with a probability of 98, 96, 94 and 92%. The results are given in Table 7 and demonstrated that the NPCHS and COE are reduced and the reliability (PLS) is decreased with increasing the FOR values. By increasing the FOR, the operational probability of the clean production resources has decreased. Therefore, to ensure the level of base reliability, the overall power level of the system must be increased, which increases the system costs but in this condition, the reliability cannot meet the reliability level of base study (without FOR).

The effect of FOR variations for photovoltaic and hydrokinetic resources are individually demonstrated in hybrid PV/HKT/FC

Table 2
The parameters used in the studied system (Jahannoosh et al., 2020; Arabi-Nowdeh et al., 2021; Naderipour et al., 2021).

Items	Value	Items	Value
PV rated size (kW)		Elecytrolyzer rated size (kg)	1
PV capital cost ($/unit)	2000	Elecytrolyzer capital cost ($/unit)	2000
PV operation and maintenance cost ($/unit-yr)	33	Elecytrolyzer operation and maintenance cost ($/unit-yr)	100
PV replacement cost ($/unit)	500	Elecytrolyzer replacement cost ($/unit)	1400
PV lifetime	20	Elecytrolyzer efficiency (%)	74
PV MPPT efficiency (%)	95	Elecytrolyzer life time	5
Reference irradiance for PV (W/m^2)	1000	Fuel cell rated size (kg)	1
Reference temperature for PV (° C)	25	Fuel cell capital cost ($/unit)	2000
Hydrokinetic rated size (kW)	10	Fuel cell O&M ($/unit-yr)	1400
Hydrokinetic capital cost ($/unit)	25000	Fuel cell replacement cost ($/unit)	100
Hydrokinetic operation and maintenance cost ($/unit-yr)	200	Fuel cell efficiency (%)	50
Hydrokinetic replacement cost ($/unit)	17000	Fuel cell life time	5
Hydrokinetic lifetime	20	Inverter rated size (kg)	1
Hydrogen tank rated size (kg)	1	Inverter capital cost ($/unit)	800
Hydrogen tank capital cost ($/unit)	1300	Inverter operation and maintenance cost ($/unit-yr)	200
Hydrogen tank operation and maintenance cost ($/unit-yr)	25	Inverter replacement cost ($/unit)	8
Hydrogen tank replacement cost ($/unit)	200	Inverter life time	15
Hydrogen tank efficiency (%)	95	Inverter efficiency (%)	90
Hydrogen tank life time	20	Total load demand (MWh)	277.78

system sizing in Figs. 20–22. As can be seen, considering the FOR for hydrokinetic compared to photovoltaic resources is more sensitive to cost increase and undermining the reliability. In other words, considering the FOR of hydrokinetic compared to the photovoltaic source's FOR will further increase energy generation costs (NPCHS and COE) and further reduce the level of reliability (PLS). The results also showed that the effect of considering the FOR of clean production resources is almost linear behavior on the system cost and reliability.

3.5. Comparison of the results

A comparison is presented with previous studies is in hybrid system sizing in Table 8. The COE ($/kWh) is given for some last researches with different algorithms, environmental information, and areas. The COE is selected as a measure for the implementation feasibility of the hybrid systems in different regions with different environmental information. Therefore, the environmental information of each region and also sizing methodology is very effective in value of this cost factor. In Borhanazad et al. (2014), PV/WT/Diesel/Battery sizing and in (Al-Sharafi et al., 2017) PV/FC/Battery system sizing is developed in different regions. The COE for studies developed in Borhanazad et al. (2014) and Al-Sharafi et al. (2017) is obtained 1.87 $/kWh and 1.40 $/kWh, respectively. The COE by the proposed methodology is achieved without FOR, with photovoltaic FOR (8%) and with hydrokinetic FOR (8%) equal to 1.57 $/kWh, 1.63 $/kWh and 1.66 $/kWh, respectively. The results showed that the cost of per kWh supply the load in this proposed methodology is higher than the PV/FC/Battery sizing in Al-Sharafi et al. (2017). Also, the cost of per kWh supply the load using the HHO is lower than the PV/WT/Diesel/Battery system sizing in Borhanazad et al. (2014).

4. Conclusion

In solving the sizing problem of the autonomous hybrid energy system, cost as economic objective function and reliability as technical constraint are considered to determine the optimal size of system components to stable supply the load. In this study, a sizing framework is developed with a meta-heuristic algorithm for different configurations of the autonomous hybrid PV/HKT/FC system with the hydrogen storage with real data of the Gorgan region considering the FOR of clean production resources. The sizing objective function is defined by minimizing the COE and reliability constraint is presented as satisfying the PLSmin. The HHO algorithm is applied to determine the optimal size of the

Table 3
Results of cost and reliability with different configurations and optimization methods with $PLS_{min} = 95\%$ considering statistic analysis.

System configuration	Item	HHO	PSO	GA	GWO
PV/HKT/FC					
	Best (USD)	**4.821**	4.916	4.912	5.063
	Mean (USD)	4.861	5.022	4.993	5.151
	Worst (USD)	4.974	5.138	5.116	5.255
	Std. (USD)	0.044	0.089	0.075	0.0683
	NPCHS	**4.821**	4.916	4.962	5.063
	COE	**1.57**	1.60	1.61	1.66
	PLS	**96.80**	96.72	96.74	96.70
PV/FC					
	Best (USD)	**8.778**	8.954	8.883	9.371
	Mean (USD)	8.562	8.766	8.657	9.164
	Worst (USD)	8.814	9.110	8.962	9.292
	Std. (USD)	0.042	0.086	0.060	0.072
	NPCHS	**8.778**	8.954	8.883	9.371
	COE	**2.86**	2.90	2.88	3.01
	PLS	**96.13**	96.04	96.10	96.06
HKT/FC					
	Best (USD)	**5.054**	5.785	5.422	5.833
	Mean (USD)	5.098	5.816	5.461	5.910
	Worst (USD)	5.128	5.947	5.780	5.947
	Std. (USD)	0.055	0.091	0.083	0.059
	NPCHS	**5.054**	5.785	5.422	5.833
	COE	**1.65**	1.89	1.78	1.91
	PLS	**95.82**	95.79	95.67	95.54

Table 4
Performance of the algorithms under multiple solutions (NPCHS values) in sizing of hybrid PV/HKT/FC system with PLS^{min}=95%.

Run	HHO	PSO	GA	GWO
1	4.849	5.017	5.106	5.182
2	4.830	5.116	5.084	5.097
3	4.864	4.934	4.933	5.255
4	4.864	5.138	4.977	5.097
5	4.846	5.017	4.962	5.224
6	**4.821**	4.944	4.962	5.240
7	4.846	5.122	4.951	**5.063**
8	4.830	4.905	5.116	5.131
9	4.846	4.934	**4.912**	5.240
10	4.830	5.122	4.977	5.131
11	4.854	4.944	4.912	5.082
12	4.830	**4.916**	4.926	5.140
13	4.846	4.981	4.933	5.063
14	4.950	5.138	5.106	5.224
15	4.974	5.122	4.951	5.240
16	4.846	4.944	4.977	5.182
17	4.893	5.122	5.116	5.182
18	4.830	5.107	4.962	5.063
19	4.830	4.944	4.926	5.097
20	4.950	4.975	5.084	5.097

system configurations considering the COE and PLSmin. The main findings are as follows:

- In the base study, the sizing of different configurations of the autonomous system such as PV/FC, HKT/FC, and PV/HKT/FC system is solved. The obtained results cleared that the PV/HKT/FC system is the best configuration with minimum COE and better PLS in comparison with the other configurations. Also, the results revealed that the system integrated with hydrokinetic more reduces the system cost and more improve the reliability compared to the system integrated with photovoltaic resources. The cost contribution of the system components demonstrated that more system cost is related to the electrolyzer (52.35%) and less cost is belongs to inverter device (1.01%). The COE is obtained 1.57 $/kWh, 2.86 $/kWh and 1.65 $/kWh and also the PLS is calculated 96.80%, 96.13% and 95.82% in sizing of the PV/HKT/FC, PV/FC and HKT/FC configurations, respectively.
- The results cleared that reducing the PLSmin causes reduction of the COE and also weakening the system reliability. The COE is changed from 1.57 $/kWh to 1.25 $/kWh due to a 15% reduction of the PLSmin value or reliability weakness.
- The sizing problem is implemented considering the FOR for optimal PV/HKT/FC configuration. The finding results

Table 5
Results of sizing with different configurations and optimization methods with PLS^{min}=95%.

System configuration	Index	HHO	PSO	GA	GWO
PV/HKT/FC					
	$P_{hydrokinetic}$ (kW)	300.16	310.29	287.73	301.27
	$P_{photovoltaic}$ (kW)	87.23	94.33	123.06	88.11
	$P_{electrolyzer}$ (kW)	321.45	335.32	337.85	332.38
	$Mass_{Tank}$ (kg)	405.28	367.41	407.91	427.03
	$P_{fuelcell}$ (kW)	17.18	16.96	15.25	18.16
	$P_{inverter}$ (kW)	48.59	48.54	48.55	48.53
PV/FC					
	$P_{hydrokinetic}$ (kW)	–	–	–	–
	$P_{photovoltaic}$ (kW)	885.23	903.16	893.85	942.64
	$P_{electrolyzer}$ (kW)	796.77	814.60	820.31	868.12
	$Mass_{Tank}(kg)$	81.16	84.79	87.62	90.87
	$P_{fuelcell}$ (kW)	16.55	16.27	15.91	16.46
	$P_{inverter}$ (kW)	48.24	48.20	48.23	48.21
HKT/FC					
	$P_{hydrokinetic}$ (kW)	398.78	507.55	452.79	383.15
	$P_{photovoltaic}$ (kW)	–	–	–	–
	$P_{electrolyzer}$ (kW)	332.31	431.34	386.63	317.59
	$Mass_{Tank}$ (kg)	446.79	167.78	271.55	470.04
	$P_{fuelcell}$ (kW)	16.94	17.49	17.55	16.76
	$P_{inverter}$ (kW)	48.09	48.07	48.01	47.95

Table 6
Numerical results of cost, reliability and sizing of PV/HKT/FC system design considering PLS^{min} variations effect.

Index	PLS^{min}=80%	PLS^{min}=85%	PLS^{min}=90%	$PLS^{\mathbf{min}}$=95%
NPCHS	3.349	3.692	4.158	4.821
COE	1.25	1.32	1.42	1.57
PLS	83.71	87.31	91.33	96.80
$P_{hydrokinetic}$ (kW)	300.33	328.32	356.83	300.16
$P_{photovoltaic}$ (kW)	0.0	0.0	4.50	87.23
$P_{electrolyzer}$ (kW)	232.77	256.09	284.85	321.45
$Mass_{Tank}$ (kg)	121.14	140.10	232.57	405.28
$P_{fuelcell}$ (kW)	16.08	17.49	17.05	17.18
$P_{inverter}$ (kW)	42.02	43.83	45.85	48.59

demonstrated that the COE is reduced and the PLS is weakened with increasing the FOR values due to reducing the operational probability of the photovoltaic and hydrokinetic resources. In a way, for the PV/HKT/FC sizing, the COE without and with FOR (8%) for hydrokinetic and photovoltaic are obtained 1.57, 1.66, and 1.63 $/kWh, and the PLS is found 96.80%, 95.43%, and 95.64%, respectively. So, the superior ability of the HHO is proved compared with the PSO, GA, GWO, and previous studies in achieving lower COE.

- Obtaining very accurate hourly data of irradiance, temperature, water flow data, and load demand data and also a large number of random optimization variables are hybrid system sizing limitations which have been extracted with great accuracy in this study. A comprehensive sizing framework for the hybrid energy system is suggested considering different algorithms and also several economic, technical, environmental, and social criteria for future work.

CRediT authorship contribution statement

Abdulaziz Alanazi: Conceptualization, Methodology, Software, Writing – original draft. **Mohana Alanazi:** Conceptualization, Methodology, Software, Writing – original draft. **Saber Arabi Nowdeh:** Writing, Investigation. **Almoataz Y. Abdelaziz:** Investigation, Supervision, Validation, Writing – review & editing. **Adel El-Shahat:** Investigation, Supervision, Methodology, Validation, Writing – review & editing.

Declaration of competing interest

The authors declare that they have no known competing financial interests or personal relationships that could have appeared to influence the work reported in this paper.

Acknowledgments

The authors extend their appreciation to the Deputyship for Research& Innovation, Ministry of Education in Saudi Arabia for funding this research work through the project number "IF_2020_NBU_429". The authors gratefully thank the Prince Faisal bin Khalid bin Sultan Research Chair in Renewable Energy Studies and Applications (PFCRE) at Northern Border University for their support and assistance.

Table 7
Results of cost, reliability and sizing of hybrid PV/HKT/FC system design considering FOR_{PV} variations effect with $PLS^{min} = 95\%$ and HHO.

PV/HKT/FC	Item	$FOR_{PV} = 0\%$	$FOR_{PV} = 2\%$	$FOR_{PV} = 4\%$	$FOR_{PV} = 6\%$	$FOR_{PV} = 8\%$
	NPCHS	4.821	4.844	4.871	4.895	4.934
	COE	1.57	1.58	1.60	1.61	1.63
	PLS	96.80	95.60	95.55	95.49	95.43
	$P_{hydrokinetic}$ (kW)	300.16	358.03	367.46	373.63	419.13
	$P_{photovoltaic}$ (kW)	87.23	13.57	4.35	2.17	0.0
	$P_{electrolyzer}$ (kW)	321.45	305.15	306.62	309.94	349.32
	$Mass_{Tank}$ (kg)	405.28	497.72	499.44	497.23	381.84
	$P_{fuelcell}$ (kW)	17.18	18.14	18.57	17.96	17.07
	$P_{inverter}$ (kW)	48.59	47.98	47.96	49.93	47.89
PV/HKT/FC	Item	$FOR_{HKT} = 0\%$	$FOR_{HKT} = 2\%$	$FOR_{HKT} = 4\%$	$FOR_{HKT} = 6\%$	$FOR_{HKT} = 8\%$
	NPCHS	4.821	4.856	4.914	5.002	5.063
	COE	1.57	1.59	1.61	1.64	1.66
	PLS	96.80	96.08	95.87	95.73	95.64
	$P_{hydrokinetic}$ (kW)	310.16	351.63	354.26	368.60	335.95
	$P_{photovoltaic}$ (kW)	87.23	26.72	31.34	0.00	102.97
	$P_{electrolyzer}$ (kW)	321.45	305.96	308.40	313.02	359.42
	$Mass_{Tank}$ (kg)	405.28	494.54	485.20	490.39	469.45
	$P_{fuelcell}$ (kW)	17.18	17.56	17.40	17.88	17.14
	$P_{inverter}$ (kW)	48.59	48.21	48.12	48.05	48.00

Table 8
Comparison of the previous sizing studies with the proposed method.

Hybrid system	Region	COE ($/kWh)
PV/WT/Diesel/Battery (Borhanazad et al., 2014)	Nahavand, Iran	1.87
PV/FC/Battery (Al-Sharafi et al., 2017)	Jeddah, Saudi Arabia	1.40
This paper (PV/HKT/FC), without FOR	Gorgan, Iran	**1.57**
This paper (PV/HKT/FC), with PV FOR (8%)	Gorgan, Iran	**1.63**
This paper (PV/HKT/FC) with HKT FOR (8%)	Gorgan, Iran	**1.66**

References

Abdelshafy, A.M., Hassan, H., Jurasz, J., 2018. Optimal design of a grid-connected desalination plant powered by renewable energy resources using a hybrid PSO–GWO approach. Energy Convers. Manage. 173, 331–347.

Adefarati, T., Bansal, R.C., 2017. Reliability assessment of distribution system with the integration of renewable distributed generation. Appl. Energy 185, 158–171.

Al-Sharafi, A., Sahin, A.Z., Ayar, T., Yilbas, B.S., 2017. Techno-economic analysis and optimization of solar and wind energy systems for power generation and hydrogen production in Saudi Arabia. Renew. Sustain. Energy Rev. 69, 33–49.

Allan, R.N., 2013. Reliability Evaluation of Power Systems. Springer Science & Business Media.

Alshammari, N., Asumadu, J., 2020. Optimum unit sizing of hybrid renewable energy system utilizing harmony search, Jaya and particle swarm optimization algorithms. Sustainable Cities Soc. 60, 102255.

Anoune, K., Bouya, M., Astito, A., Abdellah, A.B., 2018. Sizing methods and optimization techniques for PV-wind based hybrid renewable energy system: A review. Renew. Sustain. Energy Rev. 93, 652–673.

Arabi-Nowdeh, S., Nasri, S., Saftjani, P.B., Naderipour, A., Abdul-Malek, Z., Kamyab, H., Jafar-Nowdeh, A., 2021. Multi-criteria optimal design of hybrid clean energy system with battery storage considering off-and on-grid application. J. Clean. Prod. 290, 125808.

Baghaee, H.R., Mirsalim, M., Gharehpetian, G.B., Talebi, H.A., 2016. Reliability/cost-based multi-objective Pareto optimal design of stand-alone wind/PV/FC generation microgrid system. Energy 115, 1022–1041.

Borhanazad, H., Mekhilef, S., Ganapathy, V.G., Modiri-Delshad, M., Mirtaheri, A., 2014. Optimization of micro-grid system using MOPSO. Renew. Energy 71, 295–306.

De, R.K., Ganguly, A., 2021. Modeling and analysis of a solar thermal-photovoltaic-hydrogen-based hybrid power system for running a standalone cold storage. J. Clean. Prod. 293, 126202.

García, A.M., Gallagher, J., Chacón, M.C., Nabola, A.Mc., 2021. The environmental and economic benefits of a hybrid hydropower energy recovery and solar energy system (PAT-PV), under varying energy demands in the agricultural sector. J. Clean. Prod. 303, 127078.

Gharibi, M., Askarzadeh, A., 2019. Technical and economical bi-objective design of a grid-connected photovoltaic/diesel generator/fuel cell energy system. Sustainable Cities Soc. 50, 101575.

Ghorbani, N., Kasaeian, A., Toopshekan, A., Bahrami, L., Maghami, A., 2018. Optimizing a hybrid wind-PV-battery system using GA-PSO and MOPSO for reducing cost and increasing reliability. Energy 154, 581–591.

Guo, S., Liu, Q., Sun, J., Jin, H., 2018. A review on the utilization of hybrid renewable energy. Renew. Sustain. Energy Rev. 91, 1121–1147.

Hadidian-Moghaddam, M.J., Arabi-Nowdeh, S., Bigdeli, M., 2016. Optimal sizing of a stand-alone hybrid photovoltaic/wind system using new grey wolf optimizer considering reliability. J. Renew. Sustain. Energy 8 (3), 035903.

Heydari, A., Askarzadeh, A., 2016. Optimization of a biomass-based photovoltaic power plant for an off-grid application subject to loss of power supply probability concept. Appl. Energy 165, 601–611.

Jahannoosh, M., Nowdeh, S.A., Naderipour, A., Kamyab, H., Davoodkhani, I.F., Klemeš, J.J., 2020. New hybrid meta-heuristic algorithm for reliable and cost-effective designing of photovoltaic/wind/fuel cell energy system considering load interruption probability. J. Clean. Prod. 123406.

Jeyaprabha, S.B., Selvakumar, A.I., 2015. Optimal sizing of photovoltaic/battery/diesel based hybrid system and optimal tilting of solar array using the artificial intelligence for remote houses in India. Energy Build. 96, 40–52.

Kerdphol, T., Fuji, K., Mitani, Y., Watanabe, M., Qudaih, Y., 2016. Optimization of a battery energy storage system using particle swarm optimization for stand-alone microgrids. Int. J. Electr. Power Energy Syst. 81, 32–39.

Khare, V., 2019. Prediction, investigation, and assessment of novel tidal–solar hybrid renewable energy system in India by different techniques. Int. J. Sustain. Energy 38 (5), 447–468.

Kusakana, K., 2014. Techno-economic analysis of off-grid hydrokinetic-based hybrid energy systems for onshore/remote area in South Africa. Energy 68, 947–957.

Lian, J., Zhang, Y., Ma, C., Yang, Y., Chaima, E., 2019. A review on recent sizing methodologies of hybrid renewable energy systems. Energy Convers. Manage. 199, 112027.

Liu, B., Wang, Z., Feng, L., Jermsittiparsert, K., 2021. Optimal operation of photovoltaic/diesel generator/pumped water reservoir power system using modified manta ray optimization. J. Clean. Prod. 289, 125733.

Maleki, A., Nazari, M.A., Pourfayaz, F., 2020. Harmony search optimization for optimum sizing of hybrid solar schemes based on battery storage unit. Energy Rep. 6, 102–111.
Mayer, M.J., Szilágyi, A., Gróf, G., 2020. Environmental and economic multi-objective optimization of a household level hybrid renewable energy system by genetic algorithm. Appl. Energy 269, 115058.
MiarNaeimi, F., Azizyan, G., Rashki, M., 2021. Horse herd optimization algorithm: A nature-inspired algorithm for high-dimensional optimization problems. Knowl.-Based Syst. 213, 106711.
Mohamed, M.A., Eltamaly, A.M., Alolah, A.I., 2017. Swarm intelligence-based optimization of grid-dependent hybrid renewable energy systems. Renew. Sustain. Energy Rev. 77, 515–524.
Naderipour, A., Abdul-Malek, Z., Nowdeh, S.A., Kamyab, H., Ramtin, A.R., Shahrokhi, S., Klemeš, J.J., 2021. Comparative evaluation of hybrid photovoltaic, wind, tidal and fuel cell clean system design for different regions with remote application considering cost. J. Clean. Prod. 283, 124207.
Pepermans, G., Driesen, J., Haeseldonckx, D., Belmans, R., D'haeseleer, W., 2005. Distributed generation: definition, benefits and issues. Energy Policy 33 (6), 787–798.
Rajabi-Ghahnavieh, A., Nowdeh, S.A., 2014. Optimal PV–FC hybrid system operation considering reliability. Int. J. Electr. Power Energy Syst. 60, 325–333.
Sadeghi, D., Naghshbandy, A.H., Bahramara, S., 2020. Optimal sizing of hybrid renewable energy systems in presence of electric vehicles using multi-objective particle swarm optimization. Energy 209, 118471.
Sanajaoba, S., 2019. Optimal sizing of off-grid hybrid energy system based on minimum cost of energy and reliability criteria using firefly algorithm. Sol. Energy 188, 655–666.
Sanajaoba, S., Fernandez, E., 2016. Maiden application of cuckoo search algorithm for optimal sizing of a remote hybrid renewable energy system. Renew. Energy 96, 1–10.
Xu, X., Hu, W., Cao, D., Huang, Q., Chen, C., Chen, Z., 2020. Optimized sizing of a standalone PV-wind-hydropower station with pumped-storage installation hybrid energy system. Renew. Energy 147, 1418–1431.
Xu, Y.P., Ouyang, P., Xing, S.M., Qi, L.Y., Jafari, H., 2021. Optimal structure design of a PV/FC HRES using amended water Strider algorithm. Energy Rep. 7, 2057–2067.
Zhang, W., Maleki, A., Rosen, M.A., Liu, J., 2018. Optimization with a simulated annealing algorithm of a hybrid system for renewable energy including battery and hydrogen storage. Energy 163, 191–207.